future internet

MDPI

Review

Advancing Additive Manufacturing Through Machine Learning Techniques: A State-of-the-Art Review

Shaoping Xiao *, Junchao Li, Zhaoan Wang, Yingbin Chen and Soheyla Tofighi

Department of Mechanical Engineering, Iowa Technology Institute, The University of Iowa, 3131 Seamans Center, Iowa City, IA 52242, USA; junchao-li@uiowa.edu (J.L.); zhaoan-wang@uiowa.edu (Z.W.); yingbin-chen@uiowa.edu (Y.C.); soheyla-tofighi@uiowa.edu (S.T.)
* Correspondence: shaoping-xiao@uiowa.edu

Abstract: In the fourth industrial revolution, artificial intelligence and machine learning (ML) have increasingly been applied to manufacturing, particularly additive manufacturing (AM), to enhance processes and production. This study provides a comprehensive review of the state-of-the-art achievements in this domain, highlighting not only the widely discussed supervised learning but also the emerging applications of semi-supervised learning and reinforcement learning. These advanced ML techniques have recently gained significant attention for their potential to further optimize and automate AM processes. The review aims to offer insights into various ML technologies employed in current research projects and to promote the diverse applications of ML in AM. By exploring the latest advancements and trends, this study seeks to foster a deeper understanding of ML's transformative role in AM, paving the way for future innovations and improvements in manufacturing practices.

Keywords: additive manufacturing; supervised learning; semi-supervised learning; reinforcement learning

Citation: Xiao, S.; Li, J.; Wang, Z.; Chen, Y.; Tofighi, S. Advancing Additive Manufacturing Through Machine Learning Techniques: A State-of-the-Art Review. *Future Internet* **2024**, *16*, 419. https://doi.org/10.3390/fi16110419

Academic Editor: Paulo Ferreira

Received: 28 September 2024
Revised: 7 November 2024
Accepted: 12 November 2024
Published: 13 November 2024

1. Introduction

Intelligent manufacturing, or smart manufacturing, leverages advanced technologies, such as artificial intelligence (AI), machine learning (ML), the Internet of Things (IoT), robotics, automation, and big data analytics, to revolutionize production processes [1–6]. In additive manufacturing (AM), ML has transformative applications that enhance productivity, efficiency, and flexibility in production [7]. ML algorithms can drive predictive maintenance by analyzing large datasets generated at every production stage, ensuring equipment reliability and reducing downtime. ML is also pivotal in quality control, detecting defects, and ensuring consistent output in AM processes. Demand forecasting and process optimization further benefit from ML by accurately predicting material requirements, optimizing energy usage, and improving production speed. Integrating IoT devices and sensors across AM setups allows real-time monitoring, enabling ML models to adapt quickly to variations in the process or material properties, thus maintaining product quality [8,9]. Advanced robotics powered by ML can adjust to complex AM tasks, collaborating with human operators for efficient, precise assembly [10–12]. Automation in AM, coupled with ML, streamlines workflows, enhances consistency, and minimizes waste, ultimately reducing production costs [13]. These technologies enable intelligent manufacturing environments that promote agility, customization, and sustainability, reshaping traditional manufacturing into a responsive, data-driven ecosystem [14–16].

Traditional manufacturing methods like milling and turning rely on subtracting materials from a solid bulk to shape a final product [17]. In contrast, AM, often known as 3D printing, builds objects layer by layer by adding materials precisely as needed from digital designs [18,19]. This layer-by-layer approach enables AM to create complex geometries that are difficult or impossible to achieve with conventional methods, minimizes material waste, and reduces production time, allowing for faster prototyping and customization.

Key AM technologies include fused deposition modeling, stereolithography, and selective laser sintering, each offering unique advantages. For instance, fused deposition modeling, one of the most accessible techniques, uses thermoplastic filament to build layers, making it affordable and user-friendly [20]. Stereolithography, on the other hand, utilizes a UV laser to solidify photopolymer resin, yielding highly detailed parts with smooth surface finishes [21]. Selective laser sintering employs a laser to fuse powdered materials, ideal for producing durable, intricate parts from metals and ceramics [22]. Beyond these, advanced methods like direct metal laser sintering, electron beam melting, and binder jetting extend AM's potential to even more demanding applications [23–27].

AM represents a paradigm shift, promoting resource efficiency and encouraging innovation across various industries, from aerospace and automotive to healthcare and consumer goods. Enabling the synthesis of bio-inspired materials and structures opens avenues for engineering resilient, lightweight designs [28,29]. However, the scalability of AM, material constraints, and quality control present ongoing challenges that call for further research and development. Nevertheless, the technology's capacity for customization, reduced waste, and rapid production cycles signal a transformative impact on the future of manufacturing. In our view, AM has the potential to redefine sustainable manufacturing practices, aligning with both industrial needs and environmental goals in a way that traditional methods cannot fully achieve. This optimism, tempered by awareness of current limitations, underscores our belief in AM as a catalyst for future-oriented, efficient manufacturing solutions.

AI and ML stand at the crossroads of computer science, statistics, mathematics, and cognitive psychology. AI endeavors to engineer systems capable of tasks, typically requiring human intelligence, such as problem-solving, reasoning, and natural language comprehension. ML, a subset of AI, focuses on developing algorithms that enable computers to learn from data without being explicitly programmed. Within ML, supervised and unsupervised learning are prominent paradigms for processing existing data. Supervised ML, encompassing classification and regression, operates on labeled data featuring input features alongside corresponding outputs or targets.

Conversely, unsupervised ML tackles unlabeled data, exploring data structure for clustering and dimensionality reduction. Deep learning (DL), a subset of ML, harnesses neural networks with multiple layers to represent transformations and handle complex tasks, such as image recognition, natural language processing, and speech synthesis [30–33]. This methodology, characterized by its depth, has significantly advanced the field. The ML process entails identifying patterns, correlations, and statistical structures within datasets, empowering the development of intelligent systems for predictive fidelity, decision-making, and task automation. The continuous advancement of AI and ML has catalyzed breakthroughs across diverse domains, including materials science, hydrology, finance, and healthcare [34–38]. Through a combination of rigorous mathematical modeling, algorithm development, and empirical validation, scientists and engineers persistently expand the frontiers of AI and ML, unlocking new capabilities and potentials for intelligent systems.

Reinforcement learning (RL) [39], another vital subset of ML, stands as a fundamental pillar in AI, mirroring how humans learn to navigate and make decisions in a dynamic environment. Unlike supervised and unsupervised learning, RL does not rely on pre-collected datasets. Instead, the RL agent operates within an environment, iteratively exploring and learning from its experiences to achieve a specific goal through trial and error. Central to RL is the concept of reward, which provides positive or negative feedback from the environment after the agent takes action. The RL agent's objective is to learn optimal policies or strategies, guiding its decision-making process to maximize cumulative rewards over time. Reinforcement learning has diverse applications across domains like healthcare and recommendation systems [40,41]. For example, it has excelled in game-playing tasks, often surpassing human performance in chess, Go, and video games. In robotics, RL algorithms train robots to efficiently perform complex tasks, while in self-driving cars and drones, RL aids in navigation, path-finding, and decision-making [42–44].

Moreover, RL finds utility in algorithmic trading and portfolio optimization, enhancing risk management and investment decisions [45]. Smart grid systems optimize energy consumption, facilitate demand response, and integrate renewable energy resources [46]. In summary, RL presents promising solutions for addressing complex real-world challenges where explicit instruction or exhaustive search methods are impractical. Reinforcement learning's adaptability and learning capabilities make it a versatile tool for tackling diverse problems across multiple domains.

Several reviews have examined the applications of ML in the AM domain [47]. Meng and co-workers provided a thorough overview of supervised and unsupervised ML tasks in AM, focusing on parameter optimization and anomaly detection [48]. They explored regression, classification, and clustering techniques, delving into their roles in enhancing AM processes. In their analysis of regression models, the authors highlighted neural networks and Gaussian process regression as significant tools for parameter optimization, property prediction, and geometric deviation control [49–51]. Notably, with its probabilistic characteristics, Gaussian process regression offers the ability to quantify uncertainty—an essential feature in AM applications [52]. The authors discussed popular ML methods like decision trees, support vector machines (SVM), and convolutional neural networks (CNN) for classification tasks related to quality assessment, quality prediction, and defect detection [53–55]. They also addressed challenges such as model overfitting and proposed solutions to ensure robust performance. Moreover, the authors tackled the issue of dataset size limitations in AM by exploring clustering analysis methods such as the self-organizing map (SOM) model and the least absolute shrinkage and selection operator (LASSO) model. These techniques can effectively handle datasets with constrained sizes, a common challenge in AM research. Overall, this work offered valuable guidance for ideating ML applications, understanding different ML tasks, and selecting appropriate ML models in the AM domain. By synthesizing insights from various ML approaches, their review contributes to advancing the integration of ML techniques in AM processes.

In another comprehensive review, Kuman et al. focused on the applications of ML and data mining techniques in AM design, processes, and production control [56]. They initially summarized the digitization in manufacturing within the framework of Industry 4.0, which encompasses smart factories, cyber-physical systems, IoT, and AI [57,58]. Then, the authors provided an overview of supervised learning, including Bayesian networks, artificial neural networks (ANN), ensemble methods, and CNN. Additionally, they highlighted the role of generative adversarial networks (GAN) alongside CNN in assisting topology design with optimal structures [59]. Modern ML approaches have been employed for synthesizing metamaterials for material design in AM [60]. For AM processes, they reviewed various works utilizing SVM in process parameter optimization, long short-term memory (LSTM) in process monitoring, CNN in geometric deviation control, and LASSO in cost estimation, as well as other works in quality prediction, defects assessment, and closed-loop control [61–63]. They also outlined the applications of ML in AM planning, quality control, and printability and dimensional deviation management [64–66]. Additionally, the authors addressed the unique challenge of data security in AM production. They discussed uncertainty in AM through experiment-based uncertainty quantification (UQ) of the AM process, melting pool, and solidification [67,68]. In their conclusion, the authors emphasized the integration of AM and ML as a pivotal innovation in the context of the fourth industrial revolution.

The reviews mentioned above primarily concentrated on one subset of ML, supervised learning, and its applications to advance AM processes and production. However, they overlooked semi-supervised learning and RL, other crucial ML subsets known for their advantages in data mining and optimizing and controlling autonomous systems. Furthermore, the rapid accumulation of literature publications in the AM domain warrants an exploration of more recent pioneering studies. Hence, this study will present a state-of-the-art review of ML in the AM domain, emphasizing recent groundbreaking research and the applications of semi-supervised learning and RL. The structure of this paper is outlined

below: Section 2 describes ML techniques. Subsequently, recent pioneering applications of ML and RL in AM are individually reviewed, culminating in the conclusion.

2. Machine Learning

Table 1 provides a general comparison of supervised learning, semi-supervised learning, and reinforcement learning, while Table 2 outlines their respective pros and cons. The subsequent subsections will provide more detailed explanations of these three ML approaches.

Table 1. A general comparison of supervised learning, semi-supervised learning, and reinforcement learning.

Aspect	Supervised Learning	Semi-Supervised Learning	Reinforcement Learning
Definition	Learning from a labeled dataset, where each input has a corresponding output.	Combines a small amount of labeled data with a large amount of unlabeled data to improve learning.	Learning through interactions with an environment, using feedback in the form of rewards.
Training data	Requires large amounts of labeled data.	Uses a combination of labeled and unlabeled data.	Uses labeled data collected from sequential actions and rewards.
Type of problem	Regression and classification problems	Scenarios where labeling all data is expensive	Decision-making tasks for optimization and control
Learning process	Learns from input-output pairs to minimize the loss function.	Utilizes labeled data for learning and unlabeled data for structure discovery	Learns optimal policies through trial and error, maximizing cumulative rewards
Output	A model that maps inputs to outputs	A model that improves predictions	A policy that dictates the best action to take in a given state of the environment
Applications	Image recognition, sentiment analysis, predictive maintenance, medical diagnosis, etc.	Web content classification, speech recognition, natural language processing, image labeling, etc.	Robotics, self-driving cars, autonomous control systems, stock market trading, etc.

Table 2. Pros and cons of supervised learning, semi-supervised learning, and reinforcement learning.

	Supervised Learning	Semi-Supervised Learning	Reinforcement Learning
Pros	(a) Highly accurate with large, labeled data. (b) Well-suited for clear, static problems.	(a) Requires fewer labeled samples, reducing labeling costs. (b) Leverages the structure of unlabeled data to improve model performance.	(a) Good for dynamic, complex decision-making. (b) Continuously improves policies by interacting with the environment. (c) Suitable for learning in uncertain environments.
Cons	(a) Requires large amounts of labeled data, which can be expensive and time-consuming. (b) Struggles in scenarios where the data are noisy or ambiguous.	(a) Still requires some labeled data. (b) Performance may degrade if the model relies too heavily on unlabeled data. (c) Balancing labeled and unlabeled data is challenging.	(a) High computational cost due to the need for exploration. (b) Training can be unstable and slow. (c) Difficult to apply to tasks where rewards are sparse or delayed.

2.1. Supervised Learning

Supervise learning requires a pre-collected dataset to train predictive ML models, with the data labeled with output variables. It can be categorized into two types: regression and classification, depending on the nature of the output targets. Various ML models are available for supervised learning. For regression problems, options include linear and polynomial regression, while logistic regression is commonly used for classification tasks. Other methods, such as SVMs, multi-layer perceptron (MLP), decision trees, and k-nearest neighbors, have variations tailored for handling both regression and classification tasks [69]. These ML algorithms are often referred to as "shallow" because they typically involve only one layer of non-linear transformation to map input features to outputs. For instance, Aoyagi et al. proposed a framework for constructing a process map for AM [61]. They integrated a decision function, representing the porosity density of parts fabricated by AM, into SVM to predict process conditions (good or bad) based on the observations from the parts' surface. This method was shown to be effective in customizing optimized process conditions with a reduced number of experiments. However, shallow ML algorithms generally have a limited capacity to capture complex patterns in data and are often used for simple tasks.

In contrast, DL models or neural networks with multiple layers of transformations on input features become necessary when dealing with large or complex datasets [70]. One commonly used DL model is the artificial neural network (ANN) or fully connected neural network, which comprises an input layer, one or more hidden layers, and an output layer, as shown in Figure 1. The input data are fed into the input layer, where each node represents an input feature. Subsequently, the data passes through the hidden layers successively. Each layer applies weighted connections and activation functions to transform the input data into a more abstract representation. Notably, each neuron in a hidden layer is connected to all neurons in the previous and subsequent layers, rendering the neural network fully connected. Commonly used activation functions include the sigmoid function, rectified linear unit (ReLU), radial basis function (RBF), and the tangent hyperbolic function [71,72]. The final layer of the network is the output layer, which is responsible for predicting the output targets. The number of nodes in this layer depends on the dimension of the output. No activation functions are typically applied in the output layer for regression tasks, whereas the sigmoid function is used for binary classifications and the softmax function for multiclass classifications. Discrepancies between predictions based on the aforementioned feedforward process and actual outputs result in a so-called loss function. Network training aims to determine proper neuron weights to minimize this loss function. This optimization process involves backpropagation to iteratively update network weights using the gradient descent method or its variations. It is worth mentioning that physics-informed neural networks have recently garnered attention by incorporating physical laws into neural network training [73]. Consequently, the loss function comprises data loss and physics loss calculated from differential equations.

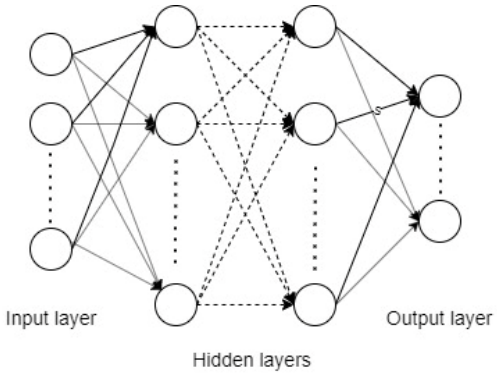

Figure 1. The architecture of an ANN.

CNNs constitute a unique class of DL algorithms specifically tailored to process and analyze data with a grid-like topology [31]. Their most prevalent application lies in image processing for computer vision tasks, where images are typically represented as grids of pixels. However, CNNs are versatile and capable of handling various other data types, including videos, two-dimensional grid geological data, three-dimensional volumetric data, and text structured as a one-dimensional grid. A typical CNN architecture (shown in Figure 2) comprises convolutional, max-pooling, and fully connected layers, collectively processing input data to make predictions for either regression or classification. Convolutional layers utilize sets of learnable filers or kernels that traverse the input data, performing element-wise multiplication and summation operations, followed by non-linear activation functions. These operations yield feature maps that capture intricate patterns and feature presentations within the input data. Max-pooling layers are often employed after convolutional layers to downsample the feature maps, effectively reducing the spatial dimensions of the data. Subsequently, the flattened feature maps, as a one-dimensional array, are passed through fully connected layers whose architecture mirrors that of ANNs, for prediction. During training, the weights and biases of a CNN are iteratively adjusted using optimization algorithms such as gradient descent and backpropagation. This adjustment process minimizes the disparity between predicted outputs and actual targets, enhancing the models' performance.

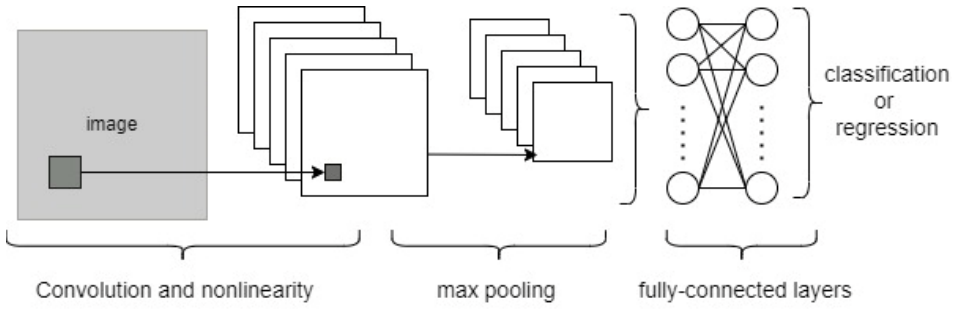

Figure 2. The architecture of a CNN.

Recurrent neural networks (RNNs) constitute another vital class of DL algorithms tailored for handling sequential data, such as text [74]. Unlike standard ANNs, which process a sequence of inputs independently, RNNs maintain an internal state to retain the memory of past inputs. This dynamic temporal behavior allows them to manage sequences of varying lengths effectively. By sharing network weights across different time steps, RNNs excel at learning patterns within sequential data, making them particularly useful in Natural Language Processing (NLP) tasks like speech recognition and text generation. Furthermore, when combined with CNNs, RNNs can even process video data from time-series images. However, traditional RNNs encounter a significant hurdle known as the vanishing gradient problem, where gradients diminish exponentially over long sequences, making it challenging to learn long-term dependencies [75]. To mitigate this issue, innovative architectures like long short-term memory (LSTM) and gated recurrent units (GRUs) have been developed [76,77]. LSTMs employ specialized gates—input, forget, and output gates—to regulate the flow of information into and out of the memory cells, facilitating selective retention or discard of information over time. On the other hand, GRUs, while similar to LSTMs, feature a simplified structure with only two gates: an update gate and a reset gate. Recently, the transformer architecture has emerged as a groundbreaking solution to the limitations of RNNs and CNNs in processing sequential data [78]. Transformers rely exclusively on self-attention mechanisms to weigh the importance of different input elements when generating outputs. This approach enables transformers to capture long-range dependencies in data more effectively than RNNs and CNNs. Transformers have achieved remarkable success across various NLP tasks, including machine translation and question-answering.

2.2. Semi-Supervised Learning

Semi-supervised learning occupies a middle ground between two well-established paradigms: supervised learning, which operates on labeled data samples to establish input-output mappings; and unsupervised learning, which discerns patterns or structures within unlabeled data [79]. In semi-supervised learning, a model is trained using a dataset comprising labeled and unlabeled samples. The labeled data aids in refining predictions, while the unlabeled data assists in developing more robust representations of the underlying data structure, thereby enhancing the model's ability to generalize to new, unseen data. Consequently, the overall performance of the model can be significantly improved. Semi-supervised learning has employed various techniques, such as self-training, co-training, consistency regularization, and pseudo-labeling. These methods harness the labeled data to initialize the model and then utilize it to make predictions on unlabeled data, iteratively refining the model for enhanced performance. Table 3 compares different semi-supervised learning methods based on their primary applications, strengths, and limitations.

Table 3. Comparison of different semi-supervised learning methods.

Methods	Description	Primary Applications	Strengths	Weaknesses
Self-training	Trains a model on labeled data and then iteratively uses its won high-confidence predictions on unlabeled data as pseudo-labels to retrain.	When labeled data are limited but large amounts of unlabeled data are available.	Simple to implement; leverages model confidence in predictions.	Can propagate errors if pseudo-labels are incorrect.
Co-training	Trains two models on different, conditionally independent views of the data and uses one model's predictions to label data for the other model.	When data have multiple independent views (e.g., text and images).	Reduces overfitting; handles multi-view data well.	Requires conditionally independent views, which may not always exist.
Consistency regularization	Enforces the model to output consistent predictions for augmented versions of unlabeled data.	When data augmentations are possible and reliable.	Robust and more generalized.	Relies on effective augmentation strategies.
Pseudo-labeling	Assigns pseudo-labels to unlabeled data based on a threshold confidence score from the model.	When model confidence indicates label quality.	Simple thresholding can improve data quality.	Needs a good confidence threshold.

Self-training, a popular semi-supervised learning method, capitalizes on unlabeled data to enhance model performance [80]. Traditionally, this technique involves using an initially trained model on labeled data to generate pseudo-labels for unlabeled samples, which are then incorporated into the training set to update the model. However, this process can be time-consuming and prone to error accumulation due to incorrect pseudo-labels. Researchers have proposed several alternative solutions to address these challenges, especially mitigating error accumulation during self-training. Berthelot et al. introduced a method that averages the results of various augmentation techniques to label unlabeled data samples [81]. Other approaches have utilized confidence thresholds to control the quality of label assignments, ensuring that only strongly augmented data samples receive labels [82–84]. Additionally, curriculum labeling has been suggested as another strategy to refine the quality of pseudo-labels during model iterations [85]. Recently, an incremental self-training technique has been developed to discern the positivity of unlabeled data through clustering [86]. This method processes the model in sequential batches to enhance performance. Moreover, a sequential query list has been introduced to streamline the

process by reducing the time consumption associated with multiple clustering and queries in iterative learning. These advancements aim to make self-training more efficient and effective in leveraging unlabeled data for model improvement.

Co-training, which originated from self-training, serves as the foundation for the bifurcated method in semi-supervised learning and is readily implementable with most ML algorithms [87–89]. Initially, co-training algorithms primarily focused on multi-view learning, which involves training multiple models (referred to as learners) on distinct subsets of features or data samples [90,91]. Each model learns from labeled data and subsequently collaborates with the other models to label the unlabeled data, leveraging inter-model agreements to reduce uncertainty. Consequently, co-training enhances model generalization by fostering cooperation among multiple learners. The key steps in co-training involve view acquisition, learner differentiation, and label confidence estimation. View acquisition necessitates a delicate balance between the independence and sufficiency of split views. Learner differentiation arises from employing basic models, selecting optimization algorithms, and configuring learner parameters (i.e., model parameters). Estimating label confidence is crucial for avoiding incorrect labeling scenarios. In contrast, single-view learning in co-training does not mandate feature splitting, aiming to prevent individual models from converging into similar hypotheses. Single-view learning capitalizes on view redundancy and conditional independence, thereby providing initial models or learners with richer information from the data [92–94].

Notably, pseudo-labeling, another popular semi-supervised learning technique, combines the principles of self-training with traditional supervised learning [95]. Pseudo-labeling is effective when the model's predictions on the unlabeled data are reliable, typically when the model's confidence in its predictions is high. However, setting a confidence threshold is essential to avoid including unreliable pseudo-labels, which could degrade performance. Additionally, pseudo-labeling may not be suitable for datasets where the distribution of the labeled and unlabeled data significantly differs. By implementing these advanced techniques, self-training and pseudo-labeling can substantially improve the performance and robustness of ML models, particularly in scenarios where labeled data are scarce or expensive to obtain. Moreover, co-training has been successfully applied across various domains, demonstrating its flexibility and effectiveness in leveraging unlabeled data to improve model performance. By utilizing multiple learners and ensuring high confidence in pseudo-labels, co-training can significantly reduce the reliance on large labeled datasets, making it a valuable technique in semi-supervised learning.

2.3. Reinforcement Learning

Unlike supervised learning, RL, another subset of ML, does not rely on pre-existing datasets [39]. Instead, an RL agent (typically a computer program) learns from its experiences by interacting with its surroundings or environment, as depicted in Figure 3. A fundamental assumption in RL is that the environment is fully observable, meaning the agent can determine its environment's configuration or state through observations. Consequently, the agent can choose an action based on the current state. Upon executing the selected action, the environment transitions to another state, and the agent receives a reward as feedback. This learning process is iterative. A mathematical framework known as the Markov decision process is commonly used to describe the interaction between the agent and its environment during learning [96,97]. The key components of this framework include a state space, an action space, a transition function, and a reward function. The transition function denotes the probability of the agent moving from the current state to the next state after taking an action, while the reward function determines the feedback the agent receives during this transition. The objective of RL for an agent is to accumulate rewards, often referred to as the expected return or utility, to the maximum extent possible. The output of RL corresponds to the agent's optimal behavior function, or the optimal policy, which maps a state to the action the agent should take.

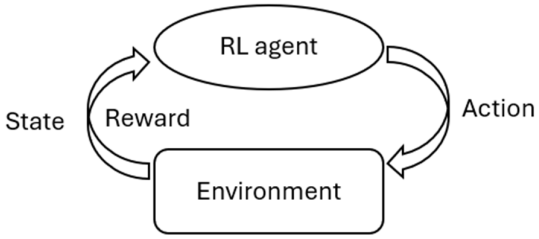

Figure 3. An RL agent learns by interacting with the environment.

There are two primary classes of methods for solving RL problems: model-based and model-free, as compared in Table 4. Model-based RL methods, such as policy iteration and value interaction, aim to determine optimal value functions using dynamic programming techniques [98]. These value functions quantify the expected return an agent can achieve from specific states or state-action pairs. The state value function represents the total reward an agent can attain starting from a particular state. Conversely, the state-action value function, also known as the action value function, indicates the expected return an agent can obtain by starting from a state and taking a specific action. Once the optimal value functions are derived, determining the optimal policy becomes feasible, as the agent tends to select actions associated with the highest values.

Table 4. Comparison between model-based and model-free RL approaches.

	Model-Based	**Model-Free**
Definition	Uses a model to simulate the environment's dynamics to predict the outcomes of actions.	Learns directly from interactions with the environment, without an internal model.
Advantages	Can plan ahead by simulating multiple steps, often requiring fewer interactions with the real environment.	Avoids the complexity of building a model, often making it more adaptable to unknown or complex environments.
Disadvantages	Requires an accurate model, which can be challenging to obtain, especially in complex environments.	Typically needs a large number of interactions with the environment, which may be costly or impractical.

Another type of RL method is model-free, which assumes that agents have no knowledge of transition probabilities and reward functions, reflecting most practical applications. Early model-free RL methods include the Monte Carlo and temporal difference methods, which are value-based RL methods. Q-learning is another widely used value-based RL method [99]. During the learning process, the agent selects the best action according to the current knowledge of the action value function at each step, receives a reward as feedback, and updates the action values through the Bellman equation [39]. It should be noted that the epsilon-greedy action selection technique is usually adopted to balance exploration and exploitation. Over many episodes, the action values converge to their optimal values, from which the optimal policy can be derived. Conventional Q-learning is a tabular method where a table stores action values with respect to the finite state and action spaces. If the state and action spaces are extremely large or continuous, an ANN can be employed to approximate action values. This method is called deep Q-Network (DQN) and is one of the methods in deep reinforcement learning (DRL) [100]. In addition to value-based RL methods, another type of model-free RL method is policy-based, as explained in Table 5. These methods directly update and converge to the optimal policy rather than the optimal value function. Policy gradient methods are a typical family of policy-based RL methods, with proximal policy optimization (PPO) being a notable example [101,102].

Table 5. Comparison between value-based and policy-based RL approaches.

	Value-Based	Policy-Based
Definition	Focuses on learning a value function (e.g., state value or action value) to estimate the expected return of actions of states.	Directly learns a policy (a mapping from states to actions) to maximize cumulative rewards.
Advantages	Often more stable and sample efficient, as it uses value functions to guide action indirectly.	Can handle continuous action spaces well and learn stochastic policies, which is beneficial in uncertain environments.
Disadvantages	May struggle with continuous action spaces and often rely on an exploration strategy.	Can be less sample efficient and prone to instability, especially in high-dimensional spaces.

3. Applications of Supervised Learning in Additive Manufacturing

Akbari et al. generated an extensive dataset and introduced a benchmark ML model for predicting mechanical properties in metal AM [103]. The dataset was sourced from over 90 metal AM articles and 140 different data sheets. The mechanical properties, including yield strength, ultimate tensile strength, elastic modulus, elongation, hardness, and surface roughness, were predicted based on processing parameters and material properties. Additionally, recent applications of supervised learning in AM include predicting the fatigue life of AM materials such as metal alloys and quality detection of AM-manufactured parts. Various ML methods, particularly DL methods, have been utilized. These methods include SVMs, ANNs, CNNs, and RNNs.

3.1. Fatigue Life Prediction

Wang et al. conducted a literature review focusing on ML-assisted fatigue life prediction of AM metallic materials [104]. They found that most studies on the fatigue life of AM parts utilized ANN models, while random forest (RF) and SVR models were applied less frequently. Additionally, most of the reviewed literature focused on stainless steel, aluminum alloy, and titanium alloy. The authors also discussed challenges and future perspectives, including difficulties in data collection, labeling, and feature engineering. Another review can be found in [105].

Table 6 presents a summary of the reviewed papers focusing on the application of supervised learning techniques for fatigue life prediction. It includes concise descriptions of the AM techniques employed in each study, the ML algorithms utilized for prediction, and the methods of data collection. These summaries aim to provide a clear understanding of the diverse approaches found in the literature. The rest of this section will explore these aspects in greater detail.

Dang et al. addressed fatigue and service life prediction in AM products using Support Vector Regression (SVR) [106]. Their study focused on thirty specimens of titanium alloy produced via the laser-directed energy deposition (LDED) method, followed by double-annealing heat treatment. Subsequently, constant-amplitude fatigue tests were conducted across three different stress levels to measure the fatigue lives, which served as labels or outputs. Microstructural analysis, facilitated by an optical microscope and scanning electron microscope (SEM), enabled the examination of the specimens for defects, particularly pores [107]. The input features in their study included the range of stress intensity near pores, pore type, the distance-size ratio (the ratio of the distance from a pore to the free surface to the equivalent diameter of the pore), pore area, and the peak stress applied on the specimen. The range of stress intensity was calculated using Murakami's approach [108], which was instrumental in evaluating stress distribution around pores. Pore type, a categorical feature, categorized pores into four types based on SEM images, considering pore size and facet visibility. Various SVR models were trained using different combinations of input features. It was found that a model incorporating two features, the

range of stress intensity and pore type, demonstrated superior performance in terms of errors and correlation coefficients. Additionally, alternative ML models, including ANNs, random forests, and Gaussian process regression, were evaluated. The comparative analysis underscored the effectiveness of the SVR model in accurately predicting fatigue life for the LDED titanium alloy specimens.

Using the ML model to predict the fatigue life of AM products requires fabricating and measuring a sufficient number of samples, which is often impractical. Recent studies have proposed incorporating physics knowledge into "black-box" ML mode to address this issue. Salvati and colleagues presented pioneering work where they developed a physics-informed neural network (PINN) or physics-informed machine learning (PIML) framework to predict the finite fatigue life of defective materials [109]. Notably, the PINN is trained using a combination of data loss and physics loss, as illustrated in Figure 4. The dataset was provided by Romano et al., who fabricated aluminum alloy samples using AM techniques like selective laser melting (SLM) [110]. These samples underwent CT scans to reconstruct the morphology and location of defects. The morphological features include the defects' volume, external surface, and the projection of the external surface onto the plane normal to the direction of the applied load. The defects' sphericity and diameter can be calculated from these features. Additionally, the distance between the defects and the free surface of the specimen can be evaluated through CT scans. Fatigue testing was conducted by applying a cyclic load of constant stress amplitudes, and the fatigue lives were measured. The samples were then investigated using fractography to detect pores, called killer defects, where fatigue cracks were triggered. In their proposed PINN framework, the neural network is enforced with phenomenological constraints from physics, specifically the linear elastic fracture mechanics (LEFM) model. In addition to the data loss from the direct prediction of the neural network, the physics loss was determined from Basquin's law for stress-fatigue life diagrams. The sum of these two loss functions was employed in the backpropagation process to optimize the network weights and bias. This research highlighted that incorporating physics laws into the neural network could be highly effective for accurately predicting the finite fatigue life of materials.

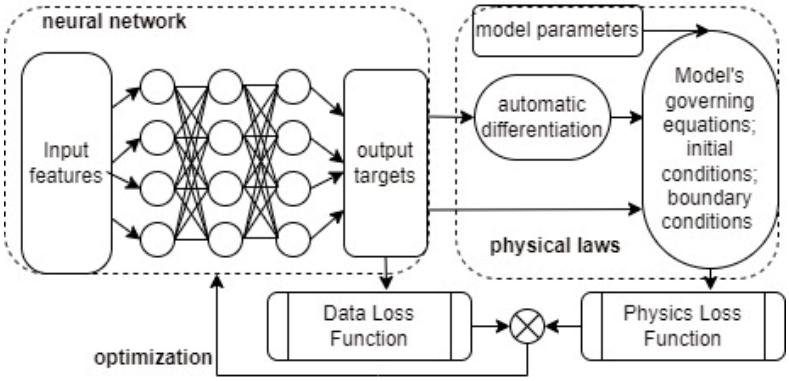

Figure 4. The training process of a PINN.

In another recent study, Wang et al. introduced physics-guided ML frameworks aimed at enhancing fatigue life prediction in AM materials [111]. Traditionally, evaluating fatigue life, particularly fatigue crack growth life, relies on Paris' law, incorporating empirical model parameters [112]. However, this physics-based model often overlooks the influence of defect characteristics such as size and location. To address this limitation, data-driven approaches like ML prove beneficial [113]. The authors employed two ML models, SVR and ANN, with inputs comprising the range of applied stress and defect features. They devised adaptive ML models using Bayesian optimization to fine-tune model hyperparameters and k-fold cross-validation for robustness. These models were trained and assessed using three different AM materials, aluminum alloy, titanium alloy, and alloy steel, across datasets varying in size from 8 to 30 [107,114,115]. Their findings suggested employing the ANN

model for scenarios with limited data and the SVR model for relatively large datasets. They also extended this physics-guided ML framework to a probabilistic model using maximum likelihood estimation. The study demonstrated that while the physics-based Paris law ensures predicted results consistent with physical observations, data-driven approaches account for the variability in fatigue lives attributed to defect features. Ultimately, the integrated physics-guided ML model maintained high prediction accuracy while mitigating overfitting issues associated with limited fatigue data.

Gao et al. explored the predictability of various ML models in forecasting the fatigue lives of titanium structures produced via AM methods, such as electron beam melting (EBM) [116]. The authors utilized experimental data [117]. The ML regression models examined in this study comprised multiple linear regression (MLR), ANNs, SVR, and random forests (RF). Initially, the study assessed the influence of density, porosity, yield stress, and fatigue stress on the predicted fatigue lives of samples. The resulting correlation matrices and heatmaps emphasized the significant impacts of yield stress and fatigue stress on the target prediction. Consequently, yield stress, which exhibited a positive correlation with fatigue life, and fatigue stress, which demonstrated a negative correlation, were selected as the input features. Following the training and evaluation of those four regression models, the authors observed that all models demonstrated excellent predictive capabilities. MLR displayed superior predictive performance at a 95% confidence interval, followed by the SVR model. Furthermore, the study addressed hyperparameter tuning and generalization for each model. Specifically, for the ANN model, three or four neurons were recommended for the first hidden layer. For the SVR model, a coefficient of 0.0001 for the RBF kernel function and a regularization hyperparameter of 30 were suggested. It was also recommended that the RF model utilize three estimators with a maximum tree depth of seven.

Recently, Li and co-workers proposed a physics-informed, data-driven framework to predict the nondestructive fatigue life of laser powder bed fusion (LPBF)-processed metal parts [118]. They fabricated two sets of LPBF Ti-6Al-4V Grade 5 parts for defect characterization and fatigue testing, respectively. Various factors influencing fatigue performance were considered, including process parameters, X-ray computed tomography (XCT)-inspected defects, and fatigue test conditions. To address the challenges of time-consuming fatigue testing and the limited availability of fatigue data, they developed a multimodal transfer learning approach to investigate the relationships between process parameters, defects, and fatigue performance. In the source task, a hierarchical graph convolutional network (HGCN) was employed to classify defects based on process parameters and defect features in images. The feature embeddings learned from the HGCN were then transferred to a neural network layer for fatigue life modeling. The proposed framework was validated through numerical simulations and an experimental case study. The FI score of defect classification reached 0.96, while the fatigue life prediction yielded a mean absolute log error as low as 0.04.

In another recent work, Nasiri et al. employed ML methods to model the fatigue lifetimes in 3D-printed biomaterials [119]. They used fused deposition modeling (FDM), a popular 3D printing method, to fabricate 162 dog-bone samples for their experiments. The study investigated the influence of three key printing parameters on fatigue behavior: print speed, nozzle diameter, and nozzle temperature. By systematically varying these parameters, they aimed to understand how each factor affects the mechanical performance of the printed biomaterials. The authors conducted rotating bending fatigue tests on the samples to gather data, generating an experimental dataset for analysis. In addition to using traditional ML models such as RF and SVR, the authors incorporated extreme gradient boosting (XGBoost), a more advanced ML algorithm known for its high accuracy and efficiency. To enhance model interpretability, they employed Shapley additive explanation (SHAP), a technique allowing more precise insights into how each feature influences the model's predictions. Upon training and testing various ML methods, they found that XGBoost outperformed the others, achieving an impressive R2 score of 0.9766. Furthermore,

the SHAP analysis revealed that nozzle diameter had the most significant impact on fatigue lifetimes, suggesting that this parameter plays a critical role in the mechanical durability of the printed biomaterials. Conversely, print speed was identified as the least influential factor. These findings highlight the potential of ML-assisted modeling in optimizing the 3D printing process for enhanced material performance.

Table 6. Summary of reviewed papers on supervised learning for fatigue life prediction in AM.

Applications	AM Techniques	ML Methods	Data Collection
Fatigue and service life prediction [106]	LDED [1]	SVR models with different input features	The authors examined 30 specimens and conducted fatigue tests [107]
Fatigue life of defective materials [109]	SLM [2]	Physics-informed neural network	Five series of samples are made and tested [110]
Fatigue crack growth life prediction [111]	HRAM [3], LDED, and LMD [4]	SVR, ANN, and Bayesian optimization	Three datasets from [104,114,115]
Fatigue life prediction [116]	EBM [5]	MLR [6], ANNs, SVR, and RF	Experimental data from [117]
Nondestructive fatigue life [118]	LPBF [7]	HGCN [8], transfer learning	Two sets of parts were fabricated for testing
Fatigue lifetime modeling [119]	FDM [9]	XGBoost [10], RF, SVR	162 samples were made for fatigue testing

[1] LDED: laser-directed energy deposition; [2] SLM: selective laser melting; [3] HRAM: hybrid in situ rolled wire + arc additive manufacturing; [4] LMD: laser melting deposition; [5] EBM: electron beam melting; [6] MLR: multiple linear regression; [7] LPBF: laser powder bed fusion; [8] HGCN: hierarchical graph convolutional network; [9] FDM: fused deposition modeling; [10] XGBoost: extreme gradient boosting.

3.2. Quality Detection

Mondal and Goswami reviewed the application of AI and ML techniques to improve quality assurance in AM processes [120]. Their review focused on the use of CNN for defect detection, highlighting CNNs' capabilities in analyzing large volumes of image data to identify and classify defects in AM products accurately. They noted that CNNs are particularly effective in this domain due to their ability to learn complex patterns and features, which makes it possible to detect various defect types with high precision. In addition, Deshpande et al. examined an advanced two-stage CNN method, Faster R-CNN, which has been effectively employed for defect localization and segmentation in AM components [121]. We reviewed several studies on supervised learning for quality detection in AM, which are summarized in Table 7, followed by detailed descriptions.

Convolutional neural networks have become a standard tool for assessing the quality of parts produced through AM, particularly in scenarios where surface polishing post-processing affects wear resistance and residual stresses. Abhilash and Ahmed integrated CNN classification into the process of electrical discharge-assisted postprocessing to enhance the surface quality of AM components [122]. In their study, titanium alloys were prepared using a direct metal laser sintering 3D printer. The researchers selected the lowest discharge energy regime for polishing the samples. Images captured through an optical microscope were fed into a CNN architecture comprising five convolutional layers and a fully connected layer for prediction. This task was a multiclass classification problem, with five surface categories reflecting different levels of surface roughness. Each class had 50 data samples (images) manufactured and polished under distinct printing and process parameters. The study leveraged the pre-trained ResNet50 model to expedite model training. Subsequently, the convolutional layer weights were transferred to the proposed CNN model, with only the weights of the fully connected layer and the output layer being fine-tuned. The researchers employed a fivefold cross-validation approach during the model training, achieving an impressive overall accuracy of 96%. Notably, all

false negative predictions were confined to borderline classes, indicating the robustness of the CNN model in discerning subtle differences in surface quality.

In a separate study, Ansari et al. investigated defects in surface deformation arising from laser powder bed fusion (LPBF), which can significantly impact the mechanical and physical properties of manufactured AM parts [123]. However, previous research did not address real-time identification of surface deformation. Ansari's study proposed a novel real-time approach to classify surface deformation problems during LPBF processing using a powder bed image as the input for each data sample. Thirteen bar-like geometries were designed and printed using an EOS printer equipped with cameras and sensors to capture each layer during printing to gather data samples. The collected powder bed images were categorized as either normal or defective. The initial dataset consisted of 1022 images converted to grayscale. Since detecting defects early is crucial to halt defect propagation promptly, selecting relevant data samples yielded a final dataset comprising 239 normal and 14 defective images. Given the dataset's significant imbalance, data augmentation methods were employed. They utilized CNN to classify the images. Three distinct model architectures were developed and tested, incorporating techniques such as early stopping, learning rate variation, and employing various model evaluation metrics to refine the model. The results showcased exceptional model performance, achieving an accuracy of up to 99%. The study also concluded that employing a balanced dataset through data augmentation could lead to a more generalized and unbiased ML model.

Moreover, Banadaki et al. devised another real-time CNN model integrated into an automated grading system to oversee the fused deposition modeling process, one of the prominent AM processes [124]. They established an image acquisition system with a high-resolution camera to capture the videos during printing. Subsequently, the data were collected by converting the videos to frames representing 21 classes based on the temperature and speed settings of the AM process. The images were manually inspected to retain only those providing proper views of the printing area. Consequently, a total of 5000 images were obtained, from which a randomly selected subset of 100 images formed the testing set. They employed a CNN architecture within a DL framework, incorporating the aggregation layers, such as convolutional and pooling layers between low-level and high-level layers. Low-level layers were utilized for spatial feature extraction, while high-level layers extracted high-order features or patterns before passing them to the fully connected layers for classification. Various metrics were used to assess the developed CNN model, including accuracy, F1 score, sensitivity, and precision. Remarkably, exceptional accuracies exceeding 93% were achieved for all classes. Additionally, the F1 score indicated relatively varied accuracies among classes with different printing settings. Once the quality predictive model was developed, it was utilized to detect the significance of the defects during the 3D printing process and monitor the process's quality.

Conrad et al. designed a comprehensive end-to-end workflow for efficiently sorting AM-manufactured parts based on specific post-processing requirements [125]. The initial stage of this automated process involved image rendering, wherein synthetic images were generated from CAD models representing the AM parts. Notably, a variety of simulated camera angles were employed during rendering, accompanied by data augmentation techniques to ensure sufficient diversity in the training data. Subsequently, pre-trained image classification neural networks were adopted and fine-tuned using the training image dataset. In the final step, the trained neural network was deployed to recognize the parts, with the resulting classification recommendations presented to the user via a graphic user interface (GUI). The GUI displayed the top three class predictions for the user to assess and compare with the actual part. The authors constructed a test set comprising 30 distinct parts to evaluate the framework, yielding 1200 images. Three pre-trained CNN architectures, MobileNetV2, ResNet-50, and VGG16, were employed, with VGG16 achieving the highest average part classification accuracy [126–128]. Furthermore, the authors enhanced the industrial applicability of their workflow by integrating physics simulation into the rendering process. In an industrial case study with 215 distinct parts,

the part classification accuracies reached 99.04% for the top three predictions and 90.37% for the top one.

Recently, Toorandaz et al. integrated a photodiode sensor with ML algorithms to establish a robust framework for surface roughness classification [129]. Data were collected by printing 42 parts with 21 distinct parameter combinations through LPBF. Several ML algorithms were employed, including RF, gradient boosting, SVM, ANN, and LSTM. They found that RF resulted in superior performance, achieving a weighted F1 score of 0.71. In another study, Wang et al. employed a CNN-based segmentation process. They developed a porosity investigation strategy to examine porosity defects in AM products using micro-computed tomography (micro-CT) [130,131]. The training data included 120 manually annotated CT slices, and the analysis revealed correlations between pore size, pore sphericity, pore evolution, and the discovery of pore-free zones. Furthermore, Zhang et al. proposed a novel feature-learning engineering framework for AM quality monitoring [132]. Their approach integrated engineering knowledge with a convolutional autoencoder and incorporated 3D neighborhood models to characterize spatiotemporal variations in melt pools during AM processes.

Table 7. Some studies on supervised learning for quality detection in AM.

Applications	ML Methods	Data Collection
Surface quality classification [122]	CNN with pre-trained ResNet50 architecture	250 images taken by an Olympus optical microscope
Surface deformation defect detection [123]	CNNs with different architectures	511 images taken before and 511 images after the AM process
Failure detecting and grading [124]	CNN with pre-trained Inception-v3 architecture	5000 images captured during the printing processes
Part recognition [125]	CNN with three different pre-trained models	A large dataset generated from CAD models
Surface roughness classification [129]	RF, ANN, SVM, and LSTM	Singal data collected a photodiode sensor during printing
Porosity defects investigation [130]	Mask region-based CNN [131]	120 manually annotated CT slices
Melt pool anomaly characterization [132]	Convolutional autoencoder	5000 melt-pool images from the in situ sensing system

3.3. Process Modeling and Control

Gunasegaram et al. reviewed both conventional closed-loop control and ML-assisted approaches in metal AM [133]. They highlighted that offline ML models could optimize AM process parameters before the process begins, whereas online models can analyze in situ sensory data to detect and diagnose defects in real-time. Additionally, they proposed an ML-assisted control framework for managing defects and anomalies during AM. Zhang et al. also reviewed process optimization and in situ monitoring techniques in LPBF AM, with a particular focus on supervised learning methods [134]. ML tasks in their review include melt pool characterization, mechanical property prediction, quality regression, and classification, among others. Several recent works on applying ML to process modeling and control are summarized in Table 8, with further details provided in this subsection.

To mitigate uncertainty in the mechanical properties and quality of parts produced using fused filament fabrication (FFF), Wenzel et al. developed a DL method to enhance the AM processing system's reliability by optimizing input parameters and predicting system responses [135]. Latin hypercube sampling was employed for experimental design to explore the input feature space and generate data efficiently [136]. The DL framework comprised an RNN and an ANN. The RNN was tasked with estimating a behavior vector based on the input parameters and past observations of the system, while the ANN predicted the system responses. This approach facilitated the identification of significant

input parameters crucial for establishing a reliable AM processing system. The principle of PIML was integrated into this DL method [137]. Domain knowledge, expressed through physical laws, was utilized to initialize neural networks to learn fundamental correlations between features. This aspect was essential for the method's applicability across different FFF 3D printing systems. For practical implementation in mass production, the authors addressed the controllability of print bed adhesion. Relevant domain knowledge, including various measurements and datasets, was extracted from scientific literature and incorporated into the proposed neural networks [138]. A case study involved four 3D printers in a temperature- and humidity-controlled environment. Four hundred experiments were designed, resulting in 1273 print bed adhesion measurements, with 20% forming a testing set. Compared to a statistical approach, the proposed method exhibited a significantly lower root mean square error (RMSE), especially when limited measurements were available.

Modeling over-deposition is critical in controlling the laser metal deposition (LMD) process to prevent additional materials from melting onto the substrate. Perani et al. developed an LSTM model to simulate over-deposition, focusing on nickel alloys with various shapes deposited via LMD [139]. Data collected during and after deposition included deposition head positions, laser activation signals, melt pool images, and deposited shapes. After data fusion, several new input features were incorporated, such as deposition speed and two variables representing the geometry of deposited shapes. Sequences of input features for 20 deposition steps were fed into the LSTM to predict deposition height for the next time step. The relative errors on the testing sets ranged from 6% to 11%. The results underscored the importance of selecting simple geometries to construct the training set for modeling the LMD process. The authors intended to utilize this model in closed-loop control of deposition parameters during real-time processes, indicating its potential for practical application in enhancing LMD processing control and efficiency.

Inyang-Udoh and colleagues developed a predictive geometry control framework for jet-based AM 3D printing processes [140]. A key component of this learning and control framework was a physics-guided data-driven model, which utilized a convolutional recurrent neural network (convRNN) to forecast the height evolution of AM manufactured parts across various scenarios [141]. The convRNN model parameters were determined by training the network with data from a limited number of layers during printing. Notably, the model could be represented in dual forms, where the layer droplet input pattern became the network parameters, making the network architecture interpretable in physical terms. This model was integrated into a feedforward control scheme, with experimental findings demonstrating its superiority over state-of-the-art open-loop control methods for 3D printing processes. Furthermore, the researchers developed an online learning algorithm for the convRNN model and implemented it into a feedback control system. They also conducted stability analyses of the developed model predictive control framework using Lyapunov theorems. The physics-guided principle allowed minimal computational effort to update the convRNN model while effectively controlling the printing system in practical applications. Additionally, the online learning and feedback control strategy mitigated process uncertainties and enhanced the geometric accuracy of the printed parts.

Huang et al. developed a novel method named multi-fidelity point-cloud neural network (MF PointNN) for surrogate modeling of the melt pool, which is critical for UQ and quality control in metallic AM processes, such as electron beam AM [142]. They generated a high-fidelity (HF) dataset comprising 280 data points using finite element (FE) modeling and simulation under uncertainty. The input features included controllable and uncontrollable parameters, while the output targets represented the thermal field response. Controllable parameters included preheating temperature, electron beam power, and beam velocity. Uncertainty stemmed from uncontrolled parameters treated as random variables, such as the absorption efficiency of beam power and material and thermal properties of titanium alloy powder, including thermal conductivity, specific heat capacity, and density. Moreover, they derived a low-fidelity (LF) dataset of 280 data points from FE simulations with coarser meshes than those used for generating HF data. In the proposed

MF PointNN framework, an LF PointNN was initially trained based on the LF training samples. Subsequently, by freezing specific network coefficients of the LF PointNN, a new PointNN was fine-tuned using the HF training data. The efficacy of this method was evaluated by comparing predictions with various methods, including FE analysis, surrogate modeling using kriging and singular value decomposition (SVD), and a standard MF modeling approach using kriging and SVD [143]. The results demonstrated that the proposed method enhanced the prediction performance of 3D thermal fields while utilizing a limited number of training data samples, thereby reducing the computation cost associated with FE analysis.

Yu and co-workers investigated the stability of the cladding layer's formation during the wire arc additive manufacturing (WAAM) process, significantly influencing the final dimensional precision of WAAM weldments [144]. The experiments utilized the cold metal transfer process, examining four different welding gun offsets and a no-offset setup. Each experiment generates a dataset of 750 samples comprising temperature distribution images on the weldment sidewall as inputs. The objective was to develop a DL model for cladding layer offset recognition, constituting a multi-class classification problem. The authors employed a CNN, integrating identity maps to facilitate the training of exceptionally deep networks. The overall detection accuracy achieved an impressive 99.84%.

Most recently, Xiao et al. utilized experimental data from the National Institute of Standards and Technology (NIST) to develop an ML model that predicts the melt pool for future parts [145]. They employed a CNN to process raw melt pool images and extract high-quality data, which was then used to train an MLP in creating a data-driven melt pool model. This model can be applied to enable reliable melt pool-guided optimization in AM processes and outperform the existing neighboring effect modeling (NBEM) method regarding average relative error in predicting melt pool size. Wang et al. applied several ML models to predict compositional changes during the AM process [146], using an explainable AI technique to reveal the relationships between process conditions and these compositional changes. Additionally, Kozjiek et al. developed an efficient tool to predict melt pool temperature variations [147]. They defined physics-based features and collected 17,892 data samples from a two-color coaxial photodiode system, employing RF and XGBoost, of which XGBoost achieved an average coefficient of determination score of 0.65.

Table 8. Summary of reviewed papers on supervised learning for process modeling and control in AM.

Applications	AM Techniques	ML/Control Methods	Data Collection
Process parameter optimization [135]	FFF [1]	RNN, ANN, and PIML	1273 print bed adhesion measurements from experiments
Over-deposition modeling [139]	LMD	LSTM	Data collected during the deposition of 36 tracks
Predictive geometry control [140]	Jet-based AM	convRNN [2] and MPC [3]	Online learning
Melt pool modeling [142]	EBM	MF PointNN [4]	Data generated from finite element simulations
Cladding layer offset recognition [144]	WAAM [5]	CNN	750 temperature distribution images from experiments
Melt pool prediction [145]	Metal AM	CNN and MLP	Experimental data from NIST
Compositional change prediction [146]	LDED	ANN, RF, SVM, etc.	117 ferromanganese specimens
Melt pool temperature variation prediction [147]	LPBF	RF and XGBoost	17,892 data samples collected from a photodiode system

[1] FFF: laser-directed energy deposition; [2] convRNN: convolutional recurrent neural network; [3] MPC: model predictive control; [4] MF PointNN: multi-fidelity point-cloud neural network; [5] WAAM: wire arc additive manufacturing.

4. Applications of Semi-Supervised Learning in Additive Manufacturing

Manivannan introduced a novel semi-supervised DL approach for automatic quality inspection in AM processes, including selective laser sintering (SLS) [148]. Unlike other automated quality inspection systems that rely solely on fully supervised learning and require large amounts of labeled data or images, the proposed approach harnesses labeled and unlabeled data, thereby reducing manual labeling efforts. In this approach, a CNN was utilized, and the loss function comprised the cross-entropy of the labeled images, the cross-entropy of the pseudo-labeled images (where unlabeled images were assumed to have true labels), and an entropy regularization term representing the probabilities of unlabeled images belonging to the true class [149]. The training procedure involved three steps. Initially, only labeled data were fed into the model, and the CNN weights and biases were iteratively adjusted to minimize the loss function. Next, the output probability of each unlabeled data was predicted, and a margin criterion was applied to assign a weight to the data. Finally, combining labeled data and weighted unlabeled data formed a new training set to update the CNN model. This approach was applied to a dataset for SLS powder bed defect detection. The results demonstrated excellent model performance with an accuracy of 98%, comparable to other state-of-the-art approaches, despite using only 25% of the labeled training data samples [150]. The author successfully applied the proposed approach to other publicly available defect inspection datasets, highlighting its flexible and extensive applicability [151–154].

Numerous supervised learning endeavors have been undertaken to efficiently monitor the quality of products produced through LPBF, a metal AM technique [155–157]. Nguyen et al. proposed a semi-supervised ML approach to minimize the effort required for labeling training data samples to detect overheating in LPBF [158,159]. For data collection, they utilized a digital camera to capture layer-by-layer monitoring images of the powder bed following laser scanning or powder recoating. The images captured after laser scanning were employed to train the ML model. This model, which featured the DeepLab v3 + network with Xception as its backbone, was designed to classify characteristic appearances at the pixel level. Data augmentation techniques were applied to prevent overfitting and enhance the model's robustness. Subsequently, the classified appearances were correlated with post-process characteristics such as surface roughness, morphology, and tensile strength to ascertain the quality of LPBF products, which were categorized as anomaly-free, exhibiting a lack of fusion, or overheated. The results demonstrated that the trained ML model possessed the capability for defect detection and quality prediction across various geometries of products. The authors suggested extending this approach to other 3D printing processes. Additionally, integrating thermal history data and employing RNNs could further enhance the model's ability to predict quality and confirm the occurrence of overheated defects.

Several studies have focused on anomaly detection during AM processes using ML techniques to anticipate flaws or porosity in products [160–163]. However, many of these approaches overlooked the dynamic nature of the manufacturing process. In a novel approach, Larsen and Hooper proposed a methodology to construct a data-driven model of the LPBF process dynamics, leveraging high-speed cameras co-axial with the laser to capture real-time process signatures during material fusion [164]. By considering the process dynamics, they framed the problem as utilizing sequences of historical observations (i.e., images), process system states, and control inputs to predict residual error between the predicted and observed states at the current time, termed the dynamic signature. This method involved multiple models. An autoregressive model with additional inputs was employed to approximate the first-order Markov chain governing the evolution of the AM process. A variational autoencoder was also utilized to extract latent variables associated with the images. Principal component analysis was then applied to reduce the dimensionality of these latent variables. Subsequently, a variational RNN was developed to process sequence data from previous time steps and predict the current state. Anomaly detection was performed by computing Kullback–Leibler divergence at each time step to

assess accumulated errors. The effectiveness of this approach was evaluated across various levels of porosity in AM products, achieving an impressive receiver operating characteristic area under a curve of up to 0.999.

In a separate study, Pandiyan et al. proposed a semi-supervised approach, utilizing ML algorithms exclusively with data from the defect-free regime of LPBF processes to predict anomalies [165]. The experiments involved creating overlapping lines to contract a defect-free cube of nickel-based super alloy. Various combinations of laser power and scanning velocity were tested to induce different LPBF process regimes, encompassing phenomena such as balling, lack of fusion pores, conduction mode, and keyhole pores. Data acquisition was facilitated using acoustic sensors, which normalized acoustic emission signals. Two generative CNN architectures were developed in this work. One architecture utilized a variational autoencoder, a commonly employed technique for tasks such as image denoising, dimensionality reduction, feature extraction, image generation, machine translation, and anomaly detection [166–168]. Typically, the encoder and decoder networks can efficiently learn the data representation densely and reconstruct the original input. The other architecture was based on a GAN, consisting of a generative network and a discriminative network, designed to generate new distribution samples from the training set [169]. Both methods yielded impressive accuracies of 96% and 97% for anomaly detection, respectively.

Mattera et al. employed a semi-supervised learning approach to enable real-time anomaly detection during WAAM [170]. Their study used established process parameters to guide material deposition and collected signal data from sensors monitoring welding current and voltage. To distinguish between normal and abnormal operations, they implemented a one-class classification model, a subtype of semi-supervised learning. This model was trained exclusively on "good" data, enabling it to learn the typical patterns of the process. Any significant deviation from these learned patterns was flagged as an anomaly, indicating potential issues in the AM process. Compared to traditional anomaly detection methods, their approach improved detection performance by 30%, demonstrating its robustness in identifying real-time irregularities during WAAM operations. In another study, Lui et al. proposed a self-supervised learning model designed to inspect and assess party quality in AM processes with minimal labeled data [171]. Their approach centered around image feature extraction, focusing on capturing defect-related features within the AM process images. These extracted features were then used to generate pseudo-labels, allowing the model to undergo self-supervised learning and adapt to defect identification without extensive labeled datasets.

5. Applications of Reinforcement Learning in Additive Manufacturing

Close-loop control systems have been developed to regulate the AM processes, allowing for adjusting process parameters during production to ensure quality control. For instance, Wang et al. [172] designed a high-speed thermal sensor and a proportional–integral–derivative (PID) controller, implementing them on an LPBF testbed. They used thermal emission, measured by the thermal sensor, as feedback to the controller because it correlated with the metal pool size. The control output was an analog voltage signal representing laser power. The experiments demonstrated that this system significantly improved printing quality, assessed through microscopic imaging and 3D scanning. As an important subset of ML, RL offers advantages for handling optimization and control problems, particularly in the context of quality control and scheduling optimization of AM processes.

5.1. Quality Control

In recent years, researchers have increasingly focused on using RL to optimize process parameters in AM processes. Table 9 summarizes several recent works, with further details provided below. Dharmawan et al. proposed a model-based RL and correction framework to control multi-layer and multi-bead (MLMB) deposition in robotic WAAM [173]. The

model-based RL approach in this study was utilized to learn an optimal relationship between process inputs and print outputs. To establish the transition from one state to another after taking action (i.e., changing process inputs), the authors collected a dataset along the print path by discretizing it into waypoints with local states and actions. A Gaussian process regression model was then trained as the kriging dynamics function. Additionally, the quality of the layer's surface was periodically assessed, and the necessary corrections were made if needed. The authors experimentally demonstrated and evaluated this learning-correction framework on a robotic WAAM system, testing it with bronze and stainless steel materials. Results showed that the standard deviation of the surface height of each printed layer was significantly reduced compared to using single-bead parameters during the WAAM processes.

Knaak et al. proposed a novel analysis approach combining CNN and RL methods to monitor product quality in LPBF AM processes [174]. They employed image-based surface roughness estimation, acquiring high-dynamic-range optical images of the product's top surfaces. These images were processed through CNNs to classify surface roughness and defective areas into five categories, ranging from very low roughness to surface distortion. Transfer learning was utilized to enhance the ML model's performance. Subsequently, a model-based RL method was used to train an agent to learn the optimal policy for selecting the best LPBF process parameters based on a given state during the AM process. This study employed an MDP framework, where the applied laser power, scan velocity, mean surface roughness, and percentage of the defective area represented an MDP state. The action space consisted of process parameters, specifically laser power and scan velocity combinations to be applied in the next layer. A random forest algorithm was also used to approximate system dynamics, serving as the transition probability function in this MDP framework for LPBF processes. The agent received rewards based on the percentage of surface defects at each state, with a higher positive reward given for a smaller defective surface area. The optimal policy was learned to maximize accumulated rewards to ensure product quality.

Ogoke and Farimani presented a DRL framework to derive a versatile control policy for minimizing the likelihood of melting defects during LPBF processes [175]. In this study, they employed a model-free and policy-based RL method, PPO, in which the policy was directly optimized. The state space was defined by sequential observations of the temperature field, including nine heat maps of the local temperature distribution around the laser's current position. These heat maps were numerically encoded and fed into a fully connected neural network as the policy network to predict an action. The action space comprised various velocities or powers of the laser, while the reward was defined as the absolute error between the target melt depth and the current depth. The algorithm was trained on a simulator, acting as a virtual environment for the agent to interact in. The simulation involved modeling the heat conduction of a moving heat source, approximating the laser, within a rectangular domain. Assumptions included considering only conduction models of heat transfer, assuming thermal properties to be temperature-independent, and treating the powder bed as a solid continuum. The simulation results indicated that the errors could be reduced by up to 91%. Additionally, the authors discussed the potential for extending this method to experimental applications through the NIST AM metrology testbed [176].

Recently, Shi et al. developed another DRL framework to enhance the uniform temperature distribution during the LDED of nickel-based alloys [177]. They first created a fast and efficient temperature simulation model of the deposition process, reducing computational costs while maintaining AM processing speed. This simulation model assumed a straight-line movement of the laser beam and employed the Rosenthal equation to evaluate temperatures at different sampling points on both sides of the product [178]. In their RL framework, the continuous state space was represented by the substrate's thermal distribution, the sample's thermal distribution, and material properties. The available actions included varying laser power, scanning speed, the deposition axis, and the deposition direction. Additionally, the transition probabilities were determined by the temperature

simulation model. They employed the PPO algorithm, a policy-based RL method. Specifically, a state, presented by a three-dimensional tensor, was fed into a CNN for feature extraction before applying critic and actor networks to update the policy. Notably, after the optimal policy was learned through simulations, it was evaluated in an LDED processing environment. The results demonstrated that the derived policy improved temperature uniformity in the products, thereby enhancing their hardness.

Dharmadhikari et al. introduced an RL methodology transformed into an optimization problem for metal AM processes to ensure repeatability, control material microstructure, and minimize product defects [179]. They proposed an off-policy RL framework based on Q-learning, a value-based RL method, for the agent to learn optimal process parameters, which included combinations of laser power and scan velocity to maintain a steady melt pool depth. Specifically, the state was represented by discrete process parameters, and the actions were the parameter changes. A Q-table was maintained and updated during the learning since both state and action paces were finite. A digital twin, developed based on the Eagar–Tsai formulation, emulated the LDED environment with which the agent interacted [180]. The model calibration was conducted experimentally on an LDED system using various laser powers and scan velocities for single-track and single-layer deposits of SS316L powder on an SS304 substrate. The experimentally derived process map also served as a validation tool to evaluate the optimal process parameters learned from the RL framework. The authors investigated the effects of various hyperparameters on the learning process, including domain discretization, the exploration-exploitation tradeoff parameter, discount factor, learning rate, and number of episodes. This study emphasized RL as an alternative approach for process parameter optimization, particularly when system information or large datasets were unavailable.

Table 9. Some studies on reinforcement learning for quality control in AM.

Applications	AM Processes	RL Methods
MLMB [1] deposition control [173]	WAAM	Model-based RL methods
Process optimization for quality improvement [174]	LPBF	Model-based RL methods
Melting defect minimization [175]	LPBF	PPO (model-free and policy-based)
Temperature uniformity improvement [177]	LDED	PPO (model-free and policy-based)
Product defect minimization [179]	LDED	Q-learning (model-free and value-based)
Defect mitigation optimization [181]	FFF	G-learning (model-free)
Process parameter optimization [182]	LPBF	Q-learning (model-free and value-based)
Process control optimization [183]	WAAM	Value iteration and DDPG [2]

[1] MLMB: multi-layer and multi-bead; [2] DDPG: deep deterministic policy gradient.

In another pioneering work, Chung et al. employed a model-free RL method to achieve optimal defect mitigation strategies for quality assurance during FFF [181]. Their approach falls into the category of online learning-based methods, designed to update the model incrementally as new data becomes available rather than training it in batch mode with a pre-provided and fixed dataset. However, the limited number of samples for shape deviation during the AM process posed a challenge for the practical utilization of online RL. To address this challenge, the authors proposed a transfer learning-based solution called continual G-learning aimed at detecting and mitigating new defects during

printing while reducing the need for extensive training samples. Specifically, continual G-learning integrated both offline and online prior knowledge. Offline prior knowledge was obtained from literature or previously experimental datasets, while online knowledge was acquired during printing. Additionally, both the reward incurred in the AM process and the information cost were considered in the expected return, which was maximized as the objective. The authors designed an experimental platform to evaluate the performance of the proposed RL framework. The results demonstrated that this method significantly improved online defect mitigation in the AM process.

Mohamed et al. proposed a novel approach to optimize process parameters in metal AM processes [182]. The environmental state variables in their method included laser power, scan speed, and hatch spacing. They applied Q-learning to identify optimal parameter combinations and validated their approach through experiments on the LPBF of aluminum alloy. The results highlighted the robustness of the predicted optimal parameters, underscoring the potential of this approach for practical applications. Similarly, Mattera et al. utilized a policy-based RL approach, especially deep deterministic policy gradient (DDPG), to develop a control policy for AM processes [183]. This policy was successfully tested on a WAAM simulator, which closely approximated a realistic AM environment.

5.2. Scheduling

Wang et al. reviewed the applications of RL in manufacturing scheduling, covering areas such as job shop scheduling, flow shop scheduling, parallel machine scheduling, and single machine scheduling [184]. They highlighted the importance of carefully designing proper action and state spaces and accurately describing the scheduling environment. Designed actions could take the form of heuristics, job sequences, or scheduled operators, while state variables might encompass various types of production information. When framing the scheduling problem as a graph, the state could be defined in terms of the conditions of nodes and edges within the graph. They also discussed challenges across problem, algorithm, and application domains, emphasizing the complexity and intricacies involved in applying RL to manufacturing scheduling.

Specifically, RL has also been applied to optimize the AM scheduling of multiple machines. Alicastro et al. proposed an RL-iterated local search (ILS) meta-heuristic to achieve optimal solutions with low computational costs [185]. The scheduling problem considered in this study was based on the SLM process to increase the utilization of machines and decrease the average cost of setup and post-processing operations. The problem definition was similar to that of batch processing machine (BPM) problems. However, in an AM scheduling problem, the processing time of a job depends not only on the total volume of the parts but also on the maximum heights of those parts. The proposed ILS algorithm was based on genetic algorithms with the variable neighborhood search, using a Q-learning approach as the local search to improve solution performance. Such a local search could effectively and efficiently choose the best neighborhood to explore for optimal solutions. The computational experiments were conducted to illustrate that the developed method reached optimal solutions faster than other approaches, especially for large productions.

Ying and Lin recently investigated two-stage assembly additive manufacturing machine scheduling problems (AMMSPs), where multiple parts were produced through job batches in the production stage before being assembled into the final products in the assembly stage [186]. The authors accounted for different specifications of each part and adopted the mixed-integer linear programming (MILP) model to define the AMMSPs as optimization problems [187]. Subsequently, they proposed an RL meta-heuristic, specifically the iterated epsilon-greedy (IEG) algorithm, to balance exploration and exploitation during the scheduling optimization. The goal of the induced optimal scheduling was to reduce the makespan by placing parts in appropriate batches during the production stage and shortening the waiting time for product assembly. To demonstrate the performance of the proposed framework, they utilized the iterated greedy (IG) algorithm as a baseline on a benchmark problem, with numerical experiments and data described in previous works [188]. The

results underscored that the proposed IEG algorithm was effective, efficient, and robust in solving AM scheduling problems.

Sun et al. formulated dynamic scheduling problems as MDPs, incorporating batch processing, random order, and machine eligibility constraints [189]. They proposed an out-of-order enabled dueling deep Q-Network (O3-DDQN) approach with a reward function closely aligned with minimizing total tardiness. Experimental results demonstrated that this approach outperformed both classical scheduling rules and state-of-the-art learning methods. In another study, Yang et al. applied DRL methods for multi-laser scanning planning [190]. The objective was to maximize fabrication efficiency while maintaining the quality of AM processes. Two case studies showed that the DRL methods achieved better scheduling performance than baseline methods.

6. Conclusions and Outlooks

This review synthesizes recent advances in ML applications in AM, focusing on challenges like high data demands, limited adaptability of traditional methods, and the need for improved quality control and process optimization. AM has historically relied on supervised learning and offline heuristic methods. Still, these approaches are often constrained by resource-intensive data labeling, limited generalization, and insufficient responsiveness to diverse manufacturing scenarios. Semi-supervised learning offers promising potential to address these issues by reducing the dependency on extensive labeled datasets and enhancing model generalization. This technique is particularly relevant to AM, where labeled data can be difficult and costly to obtain. Semi-supervised learning leverages both labeled and unlabeled data, accelerating model development and enabling it to account for a broader range of production conditions, ultimately reducing costs and time requirements in AM applications.

RL presents another critical advancement for AM by enabling real-time process control and adaptability. Unlike traditional offline optimization, RL dynamically adjusts process parameters based on immediate feedback from the AM environment. This capability allows for the continuous improvement of manufacturing outcomes, leading to increased efficiency, reduced defect rates, and enhanced flexibility. The integration of RL into AM workflows could revolutionize the field by fostering production processes that are highly responsive, adaptive, and capable of handling complex scenarios.

In conclusion, exploring advanced ML techniques, particularly semi-supervised learning and reinforcement learning, represents a transformative step toward addressing key challenges in AM. These methods stand to enhance defect detection, quality assurance, process control, and optimization while also pushing the boundaries of sustainable, high-performance manufacturing. Future research and development in this area could lead to scalable solutions, making AM more efficient and accessible across diverse industries.

Author Contributions: Conceptualization, S.X.; Writing—Original Draft Preparation, S.X.; Writing—Review and Editing, J.L., Z.W., Y.C., S.T.; Supervision, S.X.; Project Administration, S.X.; Funding Acquisition, S.X. All authors have read and agreed to the published version of the manuscript.

Funding: This research was funded by the U.S. Department of Education with grant number #P116S210005.

Data Availability Statement: No new data were created or analyzed in this study.

Conflicts of Interest: The authors declare no conflicts of interest.

References

1. Wang, B.; Tao, F.; Fang, X.; Liu, C.; Liu, Y.; Freiheit, T. Smart Manufacturing and Intelligent Manufacturing: A Comparative Review. *Engineering* **2021**, *7*, 738–757. [CrossRef]
2. Yuan, C.; Li, G.; Kamarthi, S.; Jin, X.; Moghaddam, M. Trends in intelligent manufacturing research: A keyword co-occurrence network based review. *J. Intell. Manuf.* **2022**, *33*, 425–439. [CrossRef]
3. Phuyal, S.; Bista, D.; Bista, R. Challenges, Opportunities and Future Directions of Smart Manufacturing: A State of Art Review. *Sustain. Futur.* **2020**, *2*, 100023. [CrossRef]

4. Arinez, J.F.; Chang, Q.; Gao, R.X.; Xu, C.; Zhang, J. Artificial Intelligence in Advanced Manufacturing: Current Status and Future Outlook. *J. Manuf. Sci. Eng.* **2020**, *142*, 110804. [CrossRef]
5. Kim, S.W.; Kong, J.H.; Lee, S.W.; Lee, S. Recent Advances of Artificial Intelligence in Manufacturing Industrial Sectors: A Review. *Int. J. Precis. Eng. Manuf.* **2022**, *23*, 111–129. [CrossRef]
6. Yang, T.; Yi, X.; Lu, S.; Johansson, K.H.; Chai, T. Intelligent Manufacturing for the Process Industry Driven by Industrial Artificial Intelligence. *Engineering* **2021**, *7*, 1224–1230. [CrossRef]
7. Wang, J.; Ma, Y.; Zhang, L.; Gao, R.X.; Wu, D. Deep learning for smart manufacturing: Methods and applications. *J. Manuf. Syst.* **2018**, *48*, 144–156. [CrossRef]
8. Zhong, R.Y.; Xu, X.; Klotz, E.; Newman, S.T. Intelligent Manufacturing in the Context of Industry 4.0: A Review. *Engineering* **2017**, *3*, 616–630. [CrossRef]
9. Gupta, P.; Krishna, C.; Rajesh, R.; Ananthakrishnan, A.; Vishnuvardhan, A.; Patel, S.S.; Kapruan, C.; Brahmbhatt, S.; Kataray, T.; Narayanan, D.; et al. Industrial Internet of Things in intelligent manufacturing: A review, approaches, opportunities, open challenges, and future directions. *Int. J. Interact. Des. Manuf.* **2022**, 1–23. [CrossRef]
10. Fan, H.; Liu, X.; Fuh, J.Y.H.; Lu, W.F.; Li, B. Embodied intelligence in manufacturing: Leveraging large language models for autonomous industrial robotics. *J. Intell. Manuf.* **2024**, 1–17. [CrossRef]
11. Evjemo, L.D.; Gjerstad, T.; Grøtli, E.I.; Sziebig, G. Trends in Smart Manufacturing: Role of Humans and Industrial Robots in Smart Factories. *Curr. Robot. Rep.* **2020**, *1*, 35–41. [CrossRef]
12. Ribeiro, J.; Lima, R.; Eckhardt, T.; Paiva, S. Robotic Process Automation and Artificial Intelligence in Industry 4.0—A Literature review. *Procedia Comput. Sci.* **2021**, *181*, 51–58. [CrossRef]
13. Lievano-Martínez, F.A.; Fernández-Ledesma, J.D.; Burgos, D.; Branch-Bedoya, J.W.; Jimenez-Builes, J.A. Intelligent Process Automation: An Application in Manufacturing Industry. *Sustainability* **2022**, *14*, 8804. [CrossRef]
14. Wang, J.; Xu, C.; Zhang, J.; Zhong, R. Big data analytics for intelligent manufacturing systems: A review. *J. Manuf. Syst.* **2022**, *62*, 738–752. [CrossRef]
15. Li, C.; Chen, Y.; Shang, Y. A review of industrial big data for decision making in intelligent manufacturing. *Eng. Sci. Technol. Int. J.* **2022**, *29*, 101021. [CrossRef]
16. Kozjek, D.; Vrabič, R.; Rihtaršič, B.; Lavrač, N.; Butala, P. Advancing manufacturing systems with big-data analytics: A conceptual framework. *Int. J. Comput. Integr. Manuf.* **2020**, *33*, 169–188. [CrossRef]
17. Imad, M.; Hopkins, C.; Hosseini, A.; Yussefian, N.Z.; Kishawy, H.A. Intelligent machining: A review of trends, achievements and current progress. *Int. J. Comput. Integr. Manuf.* **2022**, *35*, 359–387. [CrossRef]
18. Pereira, T.; Kennedy, J.V.; Potgieter, J. A comparison of traditional manufacturing vs additive manufacturing, the best method for the job. *Digit. Manuf. Transform. Ind. Sustain. Growth* **2019**, *30*, 11–18. [CrossRef]
19. Abdulhameed, O.; Al-Ahmari, A.; Ameen, W.; Mian, S.H. Additive manufacturing: Challenges, trends, and applications. *Adv. Mech. Eng.* **2019**, *11*, 1687814018822880. [CrossRef]
20. Cano-Vicent, A.; Tambuwala, M.M.; Hassan, S.S.; Barh, D.; Aljabali, A.A.A.; Birkett, M.; Arjunan, A.; Serrano-Aroca, A. Fused deposition modelling: Current status, methodology, applications and future prospects. *Addit. Manuf.* **2021**, *47*, 102378. [CrossRef]
21. Huang, J.; Qin, Q.; Wang, J. A Review of Stereolithography: Processes and Systems. *Processes* **2020**, *8*, 1138. [CrossRef]
22. Jabri, F.; Ouballouch, A.; Lasri, L.; EL Alaiji, R. A Review on Selective Laser Sintering 3D Printing Technology for Polymer Materials. In Proceedings of the CASICAM 2022, Casablanca, Morocco, 23–24 November 2022.
23. Venkatesh, K.V.; Nandini, V.V. Direct metal laser sintering: A digitized metal casting technology. *J. Indian Prosthodont. Soc.* **2013**, *13*, 389–392. [CrossRef] [PubMed]
24. Ahn, D.G. Directed Energy Deposition (DED) Process: State of the Art. *Int. J. Precis. Eng. Manuf. Green Technol.* **2021**, *8*, 703–742. [CrossRef]
25. Galati, M. Chapter 8—Electron beam melting process: A general overview. In *Additive Manufacturing*; Pou, J., Riveiro, A., Davim, J.P., Eds.; Elsevier: Amsterdam, The Netherlands, 2021; pp. 277–301. [CrossRef]
26. Mostafaei, A.; Elliott, A.M.; Barnes, J.E.; Li, F.; Tan, W.; Cramer, C.L.; Nandwana, P.; Chmielus, M. Binder jet 3D printing—Process parameters, materials, properties, modeling, and challenges. *Prog. Mater. Sci.* **2021**, *119*, 100707. [CrossRef]
27. Elkaseer, A.; Chen, K.J.; Janhsen, J.C.; Refle, O.; Hagenmeyer, V.; Scholz, S.G. Material jetting for advanced applications: A state-of-the-art review, gaps and future directions. *Addit. Manuf.* **2022**, *60*, 103270. [CrossRef]
28. Mu, X.; Amouzandeh, R.; Vogts, H.; Luallen, E.; Arzani, M. A brief review on the mechanisms and approaches of silk spinning-inspired biofabrication. *Front. Bioeng. Biotechnol.* **2023**, *11*, 1252499. [CrossRef]
29. Mu, X.; Wang, Y.; Cuo, C.; Li, Y.; Ling, S.; Huang, W.; Cebe, P.; Hsu, H.; Ferrari, F.D.; Jiang, X.; et al. 3D Printing of Silk Protein Structures by Aqueous Solvent-Directed Molecular Assembly. *Macromol. Biosci.* **2020**, *20*, 1900191. [CrossRef]
30. Foody, G.M.; Mathur, A. Toward intelligent training of supervised image classifications: Directing training data acquisition for SVM classification. *Remote Sens. Environ.* **2004**, *93*, 107–117. [CrossRef]
31. Sharma, N.; Jain, V.; Mishra, A. An Analysis Of Convolutional Neural Networks For Image Classification. *Int. Conf. Comput. Intell. Data Sci.* **2018**, *132*, 377–384. [CrossRef]
32. Khurana, D.; Koli, A.; Khatter, K.; Singh, S. Natural language processing: State of the art, current trends and challenges. *Multimed. Tools Appl.* **2023**, *82*, 3713–3744. [CrossRef]

33. Anumanchipalli, G.K.; Chartier, J.; Chang, E.F. Speech synthesis from neural decoding of spoken sentences. *Nature* **2019**, *568*, 493–498. [CrossRef] [PubMed]
34. Xiao, S.; Hu, R.; Li, Z.; Attarian, S.; Björk, K.-M.; Lendasse, A. A machine-learning-enhanced hierarchical multiscale method for bridging from molecular dynamics to continua. *Neural Comput. Appl.* **2020**, *32*, 14359–14373. [CrossRef]
35. Xiao, S.; Li, J.; Bordas, S.P.A.; Kim, T.Y. Artificial neural networks and their applications in computational materials science: A review and a case study. *Adv. Appl. Mech.* **2023**, *57*, 1–33. [CrossRef]
36. Gurbuz, F.; Mudireddy, A.; Mantilla, R.; Xiao, S. Using a physics-based hydrological model and storm transposition to investigate machine-learning algorithms for streamflow prediction. *J. Hydrol.* **2024**, *628*, 130504. [CrossRef]
37. Hoang, D.; Wiegratz, K. Machine learning methods in finance: Recent applications and prospects. *Eur. Financ. Manag.* **2023**, *29*, 1657–1701. [CrossRef]
38. Javaid, M.; Haleem, A.; Pratap Singh, R.; Suman, R.; Rab, S. Significance of machine learning in healthcare: Features, pillars and applications. *Int. J. Intell. Netw.* **2022**, *3*, 58–73. [CrossRef]
39. Sutton, R.S.; Barto, A.G. *Reinforcement Learning: An Introduction*; The MIT Press: London, UK, 2018.
40. Yu, C.; Liu, J.; Nemati, S.; Yin, G. Reinforcement Learning in Healthcare: A Survey. *ACM Comput. Surv.* **2021**, *55*, 1–36. [CrossRef]
41. Chen, X.; Yao, L.; McAuley, J.; Zhou, G.; Wang, X. Deep reinforcement learning in recommender systems: A survey and new perspectives. *Knowl. Based Syst.* **2023**, *264*, 110335. [CrossRef]
42. Cai, M.; Xiao, S.; Li, J.; Kan, Z. Safe reinforcement learning under temporal logic with reward design and quantum action selection. *Sci. Rep.* **2023**, *13*, 1925. [CrossRef]
43. Li, J.; Cai, M.; Kan, Z.; Xiao, S. Model-free reinforcement learning for motion planning of autonomous agents with complex tasks in partially observable environments. *Auton. Agents Multi-Agent Syst.* **2024**, *38*, 14. [CrossRef]
44. Wang, Z.; Jha, K.; Xiao, S. Continual reinforcement learning for intelligent agricultural management under climate changes. *Comput. Mater. Contin.* **2024**, *81*, 1319–1336. [CrossRef]
45. Hambly, B.; Xu, R.; Yang, H. Recent advances in reinforcement learning in finance. *Math. Financ.* **2023**, *33*, 437–503. [CrossRef]
46. Li, Y.; Yu, C.; Shahidehpour, M.; Yang, T.; Zeng, Z.; Chai, T. Deep Reinforcement Learning for Smart Grid Operations: Algorithms, Applications, and Prospects. *Proc. IEEE* **2023**, *111*, 1055–1096. [CrossRef]
47. Qi, X.; Chen, G.; Li, Y.; Cheng, X.; Li, C. Applying Neural-Network-Based Machine Learning to Additive Manufacturing: Current Applications, Challenges, and Future Perspectives. *Engineering* **2019**, *5*, 721–729. [CrossRef]
48. Meng, L.; McWilliams, B.; Jarosinski, W.; Pak, H.Y.; Jung, Y.G.; Lee, J.; Zhang, J. Machine Learning in Additive Manufacturing: A Review. *JOM* **2020**, *72*, 2363–2377. [CrossRef]
49. Tapia, G.; Khairallah, S.A.; Matthews, M.J.; King, W.E.; Elwany, A.H. Gaussian process-based surrogate modeling framework for process planning in laser powder-bed fusion additive manufacturing of 316L stainless steel. *Int. J. Adv. Manuf. Technol.* **2018**, *94*, 3591–3603. [CrossRef]
50. Mozaffar, M.; Paul, A.; Al-Bahrani, R.; Wolff, S.; Choudhary, A.; Agrawal, A.; Ehmann, K.; Cao, J. Data-driven prediction of the high-dimensional thermal history in directed energy deposition processes via recurrent neural networks. *Manuf. Lett.* **2018**, *18*, 35–39. [CrossRef]
51. Francis, J.; Bian, L. Deep Learning for Distortion Prediction in Laser-Based Additive Manufacturing using Big Data. *Manuf. Lett.* **2019**, *20*, 10–14. [CrossRef]
52. Hu, Z.; Mahadevan, S. Uncertainty quantification and management in additive manufacturing: Current status, needs, and opportunities. *Int. J. Adv. Manuf. Technol.* **2017**, *93*, 2855–2874. [CrossRef]
53. Shen, Z.; Shang, X.; Zhao, M.; Dong, X.; Xiong, G.; Wang, F.Y. A Learning-Based Framework for Error Compensation in 3D Printing. *IEEE Trans. Cybern.* **2019**, *49*, 4042–4050. [CrossRef]
54. Samie Tootooni, M.; Dsouza, A.; Donovan, R.; Rao, P.K.; Kong, Z.; Borgesen, P. Classifying the Dimensional Variation in Additive Manufactured Parts From Laser-Scanned Three-Dimensional Point Cloud Data Using Machine Learning Approaches. *J. Manuf. Sci. Eng.* **2017**, *139*, 091005. [CrossRef]
55. Gobert, C.; Reutzel, E.W.; Petrich, J.; Nassar, A.R.; Phoha, S. Application of supervised machine learning for defect detection during metallic powder bed fusion additive manufacturing using high resolution imaging. *Addit. Manuf.* **2018**, *21*, 517–528. [CrossRef]
56. Kumar, S.; Gopi, T.; Harikeerhana, N.; Gupta, M.K.; Gaur, V.; Krolczyk, G.M.; Wu, C. Machine learning techniques in additive manufacturing: A state of the art review on design, processes and production control. *J. Intell. Manuf.* **2023**, *34*, 21–55. [CrossRef]
57. Ghobakhloo, M. Industry 4.0, digitization, and opportunities for sustainability. *J. Clean. Prod.* **2020**, *252*, 119869. [CrossRef]
58. Lucke, D.; Constantinescu, C.; Westkämper, E. Smart Factory—A Step towards the Next Generation of Manufacturing. In *Manufacturing Systems and Technologies for the New Frontier*; Mitsuishi, M., Ueda, K., Kimura, F., Eds.; Springer: London, UK, 2008; pp. 115–118.
59. Behzadi, M.M.; Ilieş, H.T. Real-Time Topology Optimization in 3D via Deep Transfer Learning. *Comput. Aided Des.* **2021**, *135*, 103014. [CrossRef]
60. Gu, G.X.; Chen, C.T.; Richmond, D.J.; Buehler, M.J. Bioinspired hierarchical composite design using machine learning: Simulation, additive manufacturing, and experiment. *Mater. Horiz.* **2018**, *5*, 939–945. [CrossRef]
61. Aoyagi, K.; Wang, H.; Sudo, H.; Chiba, A. Simple method to construct process maps for additive manufacturing using a support vector machine. *Addit. Manuf.* **2019**, *27*, 353–362. [CrossRef]

62. Zhang, Z.; Liu, Z.; Wu, D. Prediction of melt pool temperature in directed energy deposition using machine learning. *Addit. Manuf.* **2021**, *37*, 101692. [CrossRef]
63. Chan, S.L.; Lu, Y.; Wang, Y. Data-driven cost estimation for additive manufacturing in cybermanufacturing. *J. Manuf. Syst.* **2017**, *46*, 115–126. [CrossRef]
64. Lu, S.C.Y. Machine learning approaches to knowledge synthesis and integration tasks for advanced engineering automation. *Comput. Ind.* **1990**, *15*, 105–120. [CrossRef]
65. Kumar, S.; Wu, C. Eliminating intermetallic compounds via Ni interlayer during friction stir welding of dissimilar Mg/Al alloys. *J. Mater. Res. Technol.* **2021**, *15*, 4353–4369. [CrossRef]
66. Khanzadeh, M.; Chowdhury, S.; Tschopp, M.A.; Doude, H.R.; Marufuzzaman, M.; Bian, L. In-situ monitoring of melt pool images for porosity prediction in directed energy deposition processes. *IISE Trans.* **2019**, *51*, 437–455. [CrossRef]
67. Tapia, G.; Elwany, A.H.; Sang, H. Prediction of porosity in metal-based additive manufacturing using spatial Gaussian process models. *Addit. Manuf.* **2016**, *12*, 282–290. [CrossRef]
68. Lopez, F.; Witherell, P.; Lane, B. Dentifying Uncertainty in Laser Powder Bed Fusion Additive Manufacturing Models. *J. Mech. Des.* **2016**, *138*, 114502. [CrossRef] [PubMed]
69. Hsu, C.W.; Lin, C.J. A comparison of methods for multiclass support vector machines. *IEEE Trans. Neural Netw.* **2002**, *13*, 415–425. [CrossRef]
70. Lecun, Y.; Bengio, Y.; Hinton, G. Deep learning. *Nature* **2015**, *521*, 436–444. [CrossRef]
71. Nair, V.; Hinton, G. Rectified linear units improve restricted boltzmann machines. In Proceedings of the 27th International Conference on International Conference on Machine Learning, Haifa, Israel, 21–24 June 2010.
72. Chen, S.; Cowan, C.F.N.; Grant, P.M. Orthogonal least squares learning algorithm for radial basis function networks. *IEEE Trans. Neural Netw.* **1991**, *2*, 302–309. [CrossRef]
73. Raissi, M.; Perdikaris, P.; Karniadakis, G.E. Physics-informed neural networks: A deep learning framework for solving forward and inverse problems involving nonlinear partial differential equations. *J. Comput. Phys.* **2019**, *378*, 686–707. [CrossRef]
74. Mienye, I.D.; Swart, T.G.; Obaido, G. Recurrent neural networks: A comprehensive review of architectures, variants, and applications. *Information* **2014**, *15*, 517. [CrossRef]
75. Bengio, Y.; Simard, P.; Frasconi, P. Learning Long-Term Dependencies with Gradient Descent is Difficult. *IEEE Trans. Neural Netw.* **1994**, *5*, 157–166. [CrossRef]
76. Hochreiter, S.; Schmidhuber, J. Long Short-Term Memory. *Neural Comput.* **1997**, *9*, 1735–1780. [CrossRef] [PubMed]
77. Gruber, N.; Jockisch, A. Are GRU Cells More Specific and LSTM Cells More Sensitive in Motive Classification of Text? *Front. Artif. Intell.* **2020**, *3*, 40. [CrossRef]
78. Lin, T.; Wang, Y.; Liu, X.; Qiu, X. A survey of transformers. *AI Open* **2022**, *3*, 111–132. [CrossRef]
79. van Engelen, J.E.; Hoos, H.H. A survey on semi-supervised learning. *Mach. Learn.* **2020**, *109*, 373–440. [CrossRef]
80. Yarowsky, D. Unsupervised word sense disambiguation rivaling supervised methods. In Proceedings of the 33rd Annual Meeting on Association for Computational Linguistics, Cambridge, MA, USA, 26–30 June 1995.
81. Berthelot, D.; Carlini, N.; Goodfellow, I.; Oliver, A.; Papernot, N.; Raffel, C. MixMatch: A holistic approach to semi-supervised learning. In Proceedings of the 33rd International Conference on Neural Information Processing Systems, Vancouver, BC, Canada, 8–14 December 2019.
82. Xie, Q.; Dai, Z.; Hovy, E.; Luong, M.T.; Le, Q.V. Unsupervised data augmentation for consistency training. In Proceedings of the 34th International Conference on Neural Information Processing Systems, Vancouver, BC, Canada, 6–12 December 2020.
83. Berthelot, D.; Carlini, N.; Cubuk, E.D.; Kurakin, A.; Sohn, K.; Zhang, H.; Raffel, C. ReMixMatch: Semi-Supervised Learning with Distribution Matching and Augmentation Anchoring. In Proceedings of the International Conference on Learning Representations, Virtual, 26 April–1 May 2020.
84. Sohn, K.; Berthelot, D.; Li, C.L.; Zhang, Z.; Carlini, N.; Cubuk, E.D.; Kurakin, A.; Zhang, H.; Raffel, C. FixMatch: Simplifying semi-supervised learning with consistency and confidence. In Proceedings of the 34th International Conference on Neural Information Processing Systems, Vancouver, BC, Canada, 6–12 December 2020.
85. Cascante-Bonilla, P.; Tan, F.; Qi, Y.; Ordonez, V. Curriculum Labeling: Revisiting Pseudo-Labeling for Semi-Supervised Learning. In Proceedings of the AAAI Conference on Artificial Intelligence, Virtual, 2–9 February 2021.
86. Guo, J.; Liu, Z.; Chen, C.L.P. An Incremental-Self-Training-Guided Semi-Supervised Broad Learning System. *IEEE Trans. Neural Netw. Learn. Syst.* **2024**, 1–15. [CrossRef]
87. Blum, A.; Mitchell, T. Combining labeled and unlabeled data with co-training. In Proceedings of the Eleventh Annual Conference on Computational Learning Theory, Madison, WI, USA, 24–26 July 1998.
88. Liu, W.; Li, Y.; Tao, D.; Wang, Y. A general framework for co-training and its applications. *Neurocomputing* **2015**, *167*, 112–121. [CrossRef]
89. Ning, X.; Wang, X.; Xu, S.; Cai, W.; Zhang, L.; Yu, L.; Li, W. A review of research on co-training. *Concurr. Comput. Pract. Exp.* **2023**, *35*, e6276. [CrossRef]
90. Balcan, M.; Blum, A.; Yang, K. Co-Training and Expansion: Towards Bridging Theory and Practice. In Proceedings of the 18th International Conference on Neural Information Processing Systems, Vancouver, BC, Canada, 13–18 December 2004.
91. Nigam, K.; Ghani, R. Analyzing the effectiveness and applicability of co-training. In Proceedings of the Ninth International Conference on Information and Knowledge Management, McLean, VA, USA, 6–11 November 2000.

92. Goldman, S.A.; Zhou, Y. Enhancing Supervised Learning with Unlabeled Data. In Proceedings of the International Conference on Machine Learning, Stanford, CA, USA, 29 June–2 July 2000.
93. Zhou, Z.H.; Li, M. Tri-training: Exploiting unlabeled data using three classifiers. *IEEE Trans. Knowl. Data Eng.* **2005**, *17*, 1529–1541. [CrossRef]
94. Chen, X.; Cao, W.; Gan, C.; Ohyama, Y.; She, J.; Wu, M. Semi-supervised support vector regression based on data similarity and its application to rock-mechanics parameters estimation. *Eng. Appl. Artif. Intell.* **2021**, *104*, 104317. [CrossRef]
95. Ferreira, R.E.P.; Lee, Y.J.; Dórea, J.R.R. Using pseudo-labeling to improve performance of deep neural networks for animal identification. *Sci. Rep.* **2023**, *13*, 13875. [CrossRef]
96. Ding, X.; Smith, S.L.; Belta, C.; Rus, D. Optimal control of Markov decision processes with linear temporal logic constraints. *IEEE Trans. Autom. Control* **2014**, *59*, 1244–1257. [CrossRef]
97. van Ravenzwaaij, D.; Cassey, P.; Brown, S.D. A simple introduction to Markov Chain Monte–Carlo sampling. *Psychon. Bull. Rev.* **2018**, *25*, 143–154. [CrossRef] [PubMed]
98. Howard, R.A. *Dynamic Programming and Markov Processes*; MIT Press: Cambridge, MA, USA, 1960.
99. Watkins, C.; Dayan, P. Q-Learning. *Mach. Learn.* **1992**, *8*, 279–292. [CrossRef]
100. van Hasselt, H.; Guez, A.; Silver, D. Deep Reinforcement Learning with Double Q-Learning. In Proceedings of the Thirtieth AAAI Conference on Artificial Intelligence, Phoenix, AZ, USA, 17–23 February 2016.
101. Kakade, S.; Langford, J. Approximately optimal approximate reinforcement learning. In Proceedings of the Nineteenth International Conference on Machine Learning, Sydney, Australia, 8–12 July 2002.
102. Gu, Y.; Cheng, Y.; Chen, C.L.P.; Wang, X. Proximal Policy Optimization With Policy Feedback. *IEEE Trans. Syst. Man Cybern. Syst.* **2022**, *52*, 400–4610. [CrossRef]
103. Akbari, P.; Zamani, M.; Mostafaei, A. Machine learning prediction of mechanical properties in metal additive manufacturing. *Addit. Manuf.* **2024**, *91*, 104320. [CrossRef]
104. Wang, H.; Gao, S.L.; Wang, B.T.; Ma, Y.T.; Guo, Z.J.; Zhang, K.; Yang, Y.; Yue, X.Z.; Hou, J.; Huang, H.J.; et al. Recent advances in machine learning-assisted fatigue life prediction of additive manufactured metallic materials: A review. *J. Mater. Sci. Technol.* **2024**, *198*, 111–136. [CrossRef]
105. Javidrad, H.; Koc, B.; Bayraktar, H.; Simsek, U.; Gunaydin, K. Fatigue performance of metal additive manufacturing: A comprehensive overview. *Virtual Phys. Prototyp.* **2024**, *19*, e2302556. [CrossRef]
106. Dang, L.; He, X.; Tang, D.; Li, Y.; Wang, T. A fatigue life prediction approach for laser-directed energy deposition titanium alloys by using support vector regression based on pore-induced failures. *Int. J. Fatigue* **2022**, *159*, 106748. [CrossRef]
107. Wang, X.; He, X.; Wang, T.; Li, Y. Internal pores in DED Ti-6.5Al-2Zr-Mo-V alloy and their influence on crack initiation and fatigue life in the mid-life regime. *Addit. Manuf.* **2019**, *28*, 373–393. [CrossRef]
108. Murakami, Y. Additive manufacturing: Effects of defects. In *Metal Fatigue*, 2nd ed.; Murakami, Y., Ed.; Academic Press: Cambridge, MA, USA, 2019; pp. 453–483.
109. Salvati, E.; Tognan, A.; Laurenti, L.; Pelegatti, M.; De Bona, F. A defect-based physics-informed machine learning framework for fatigue finite life prediction in additive manufacturing. *Mater. Des.* **2022**, *222*, 111089. [CrossRef]
110. Romano, S.; Brückner-Foit, A.; Brandão, A.; Gumpinger, J.; Ghidini, T.; Beretta, S. Fatigue properties of AlSi10Mg obtained by additive manufacturing: Defect-based modelling and prediction of fatigue strength. *Eng. Fract. Mech.* **2018**, *187*, 165–189. [CrossRef]
111. Wang, L.; Zhu, S.P.; Luo, C.; Liao, D.; Wang, Q. Physics-guided machine learning frameworks for fatigue life prediction of AM materials. *Int. J. Fatigue* **2023**, *172*, 107658. [CrossRef]
112. Paris, P.; Erdogan, F. A Critical Analysis of Crack Propagation Laws. *J. Basic Eng.* **1963**, *85*, 528–533. [CrossRef]
113. He, L.; Wang, Z.; Ogawa, Y.; Akebono, H.; Sugeta, A.; Hayashi, Y. Machine-learning-based investigation into the effect of defect/inclusion on fatigue behavior in steels. *Int. J. Fatigue* **2022**, *155*, 106597. [CrossRef]
114. Xie, C.; Wu, S.; Yu, Y.; Zhang, H.; Hu, Y.; Zhang, M.; Wang, G. Defect-correlated fatigue resistance of additively manufactured Al-Mg4.5Mn alloy with in situ micro-rolling. *J. Mater. Process. Technol.* **2021**, *291*, 117039. [CrossRef]
115. Cui, X.; Zhang, S.; Wang, C.; Zhang, C.H.; Chen, J.; Zhang, J.B. Microstructure and fatigue behavior of a laser additive manufactured 12CrNi2 low alloy steel. *Mater. Sci. Eng. A* **2020**, *772*, 138685. [CrossRef]
116. Gao, S.; Yue, X.; Wang, H. Predictability of Different Machine Learning Approaches on the Fatigue Life of Additive-Manufactured Porous Titanium Structure. *Metals* **2024**, *14*, 320. [CrossRef]
117. Liu, Y.J.; Wang, H.L.; Li, S.J.; Wang, S.G.; Wang, W.J.; Hou, W.T.; Hao, Y.L.; Yang, R.; Zhang, L.C. Compressive and fatigue behavior of beta-type titanium porous structures fabricated by electron beam melting. *Acta Mater.* **2017**, *126*, 58–66. [CrossRef]
118. Li, A.; Poudel, A.; Shao, S.; Shamsaei, N.; Liu, J. Nondestructive fatigue life prediction for additively manufactured metal parts through a multimodal transfer learning framework. *IISE Trans.* **2024**, 1–16. [CrossRef]
119. Nasiri, H.; Dadashi, A.; Azadi, M. Machine learning for fatigue lifetime predictions in 3D-printed polylactic acid biomaterials based on interpretable extreme gradient boosting model. *Mater. Today Commun.* **2024**, *39*, 109054. [CrossRef]
120. Mondal, S.; Goswami, S.S. Machine learning techniques for quality assurance in additive manufacturing processes. *Int. J. AI Mater. Des.* **2024**, *1*, 21–40. [CrossRef]
121. Deshpande, S.; Venugopal, V.; Kumar, M.; Anand, S. Deep learning-based image segmentation for defect detection in additive manufacturing: An overview. *Int. J. Adv. Manuf. Technol.* **2024**, *134*, 2081–2105. [CrossRef]

122. Abhilash, P.M.; Ahmed, A. Convolutional neural network–based classification for improving the surface quality of metal additive manufactured components. *Int. J. Adv. Manuf. Technol.* **2023**, *126*, 3873–3885. [CrossRef]
123. Ansari, M.A.; Crampton, A.; Parkinson, S. A Layer-Wise Surface Deformation Defect Detection by Convolutional Neural Networks in Laser Powder-Bed Fusion Images. *Materials* **2022**, *15*, 7166. [CrossRef]
124. Banadaki, Y.; Razaviarab, N.; Fekrmandi, H.; Li, G.; Mensah, P.; Bai, S.; Sharifi, S. Automated Quality and Process Control for Additive Manufacturing using Deep Convolutional Neural Networks. *Recent Prog. Mater.* **2022**, *4*, 5. [CrossRef]
125. Conrad, J.; Rodriguez, S.; Omidvarkarjan, D.; Ferchow, J.; Meboldt, M. Recognition of Additive Manufacturing Parts Based on Neural Networks and Synthetic Training Data: A Generalized End-to-End Workflow. *Appl. Sci.* **2023**, *13*, 12316. [CrossRef]
126. Sandler, M.; Howard, A.; Zhu, M.; Zhmoginov, A.; Chen, L.C. MobileNetV2: Inverted Residuals and Linear Bottlenecks. In Proceedings of the IEEE Conference on Computer Vision and Pattern Recognition, Salt Lake City, UT, USA, 18–23 June 2018.
127. He, K.; Zhang, X.; Ren, S.; Sun, J. Deep Residual Learning for Image Recognition. In Proceedings of the IEEE Conference on Computer Vision and Pattern Recognition, Las Vegas, NV, USA, 27–30 June 2016.
128. Simonyan, K.; Zisserman, A. Very Deep Convolutional Networks for Large-Scale Image Recognition. In Proceedings of the International Conference on Learning Representations, Banff, AB, Canada, 14–16 April 2014.
129. Toorandaz, S.; Taherkhani, K.; Liravi, F.; Toyserkani, E. A novel machine learning-based approach for in-situ surface roughness prediction in laser powder-bed fusion. *Addit. Manuf.* **2024**, *91*, 104354. [CrossRef]
130. Wang, Y.; Ng, C.; Bermingham, M.; Dargusch, M. Machine learning driven instance segmentation providing new porosity insights into wire arc directed energy deposited Ti-22V-4Al. *Addit. Manuf.* **2024**, *90*, 104323. [CrossRef]
131. He, K.; Gkioxari, G.; Dollar, P.; Girshick, R. Mask R-CNN. In Proceedings of the IEEE International Conference on Computer Vision, Venice, Italy, 22–29 October 2017.
132. Zhang, S.; Yang, H.; Yang, Z.; Lu, Y. Engineering-guided deep learning of melt-pool dynamics for additive manufacturing quality monitoring. *J. Comput. Inf. Sci. Eng.* **2024**, *24*, 101002. [CrossRef]
133. Gunasegaram, D.R.; Barnard, A.S.; Matthews, M.J.; Jared, B.H.; Andreaco, A.M.; Bartsch, K.; Murphy, A.B. Machine learning-assisted in-situ adaptive strategies for the control of defects and anomalies in metal additive manufacturing. *Addit. Manuf.* **2024**, *81*, 104013. [CrossRef]
134. Zhang, J.; Yin, G.; Xu, Y.; Sing, S.L. Machine learning applications for quality improvement in laser powder bed fusion: A state-of-the-art review. *Int. J. AI Mater. Des.* **2024**, *1*, 2301. [CrossRef]
135. Wenzel, S.; Slomski-Vetter, E.; Melz, T. Optimizing System Reliability in Additive Manufacturing Using Physics-Informed Machine Learning. *Machines* **2022**, *10*, 525. [CrossRef]
136. Ye, K.Q. Orthogonal Column Latin Hypercubes and Their Application in Computer Experiments. *J. Am. Stat. Assoc.* **1998**, *93*, 1430–1439. [CrossRef]
137. Kapusuzoglu, B.; Mahadevan, S. Physics-Informed and Hybrid Machine Learning in Additive Manufacturing: Application to Fused Filament Fabrication. *JOM* **2020**, *72*, 4695–4705. [CrossRef]
138. Spoerk, M.; Gonzalez-Gutierrez, J.; Lichal, C.; Cajner, H.; Berger, G.R.; Schuschnigg, S.; Cardon, L.; Holzer, C. Optimisation of the Adhesion of Polypropylene-Based Materials during Extrusion-Based Additive Manufacturing. *Polymers* **2018**, *10*, 490. [CrossRef]
139. Perani, M.; Jandl, R.; Baraldo, S.; Valente, A.; Paoli, B. Long-short term memory networks for modeling track geometry in laser metal deposition. *Front. Artif. Intell.* **2023**, *6*, 1156630. [CrossRef]
140. Inyang-Udoh, U.; Chen, A.; Mishra, S. A Learn-and-Control Strategy for Jet-Based Additive Manufacturing. *IEEE ASME Trans. Mechatron.* **2022**, *27*, 1946–1954. [CrossRef]
141. Inyang-Udoh, U.; Mishra, S. A Physics-Guided Neural Network Dynamical Model for Droplet-Based Additive Manufacturing. *IEEE Trans. Control Syst. Technol.* **2022**, *30*, 1863–1875. [CrossRef]
142. Huang, X.; Xie, T.; Wang, Z.; Chen, L.; Zhou, Q.; Hu, Z. A Transfer Learning-Based Multi-Fidelity Point-Cloud Neural Network Approach for Melt Pool Modeling in Additive Manufacturing. *ASCE-ASME J. Risk Uncertain. Eng. Syst. Part B Mech. Eng.* **2021**, *8*, 011104. [CrossRef]
143. Shu, L.; Jiang, P.; Zhou, Q.; Shao, X.; Hu, J.; Meng, X. An on-line variable fidelity metamodel assisted Multi-objective Genetic Algorithm for engineering design optimization. *Appl. Soft Comput.* **2018**, *66*, 438–448. [CrossRef]
144. Yu, R.; He, S.; Yang, D.; Zhang, X.; Tan, X.; Xing, Y.; Zhang, T.; Huang, Y.; Wang, L.; Peng, Y.; et al. Identification of cladding layer offset using infrared temperature measurement and deep learning for WAAM. *Opt. Laser Technol.* **2024**, *170*, 110243. [CrossRef]
145. Xiao, Y.; Wang, X.; Yang, W.; Yao, X.; Yang, Z.; Lu, Y.; Wang, Z.; Chen, L. Data-driven prediction of future melt pool from built parts during metal additive manufacturing. *Addit. Manuf.* **2024**, *93*, 104438. [CrossRef]
146. Wang, J.; Kim, E.S.; Kim, H.S.; Lee, B.J. A machine learning approach for predicting evaporation-induced composition variability in directed energy deposition in-situ alloying. *Addit. Manuf.* **2024**, *92*, 104384. [CrossRef]
147. Kozjek, D.; Porter, C.; Carter, F.M., III; Mogonye, J.E.; Cao, J. Data-driven prediction of inter-layer process condition variations in laser powder bed fusion. *Addit. Manuf.* **2024**, *88*, 104230. [CrossRef]
148. Manivannan, S. Automatic quality inspection in additive manufacturing using semi-supervised deep learning. *J. Intell. Manuf.* **2023**, *34*, 3091–3108. [CrossRef]
149. Tanaka, D.; Ikami, D.; Yamasaki, T.; Aizawa, K. Joint Optimization Framework for Learning with Noisy Labels. In Proceedings of the IEEE/CVF Conference on Computer Vision and Pattern Recognition, Salt Lake City, UT, USA, 18–23 June 2018.

150. Westphal, E.; Seitz, H. A machine learning method for defect detection and visualization in selective laser sintering based on convolutional neural networks. *Addit. Manuf.* **2021**, *41*, 101965. [CrossRef]
151. Rizve, M.N.; Duarte, K.; Rawat, Y.S.; Shah, M. In Defense of Pseudo-Labeling: An Uncertainty-Aware Pseudo-label Selection Framework for Semi-Supervised Learning. In Proceedings of the International Conference on Learning Representation, Virtual, 3–7 May 2021.
152. Wang, Y.; Gao, L.; Gao, Y.; Li, X. A new graph-based semi-supervised method for surface defect classification. *Robot. Comput.-Integr. Manuf.* **2021**, *68*, 102083. [CrossRef]
153. Xu, L.; Lv, S.; Deng, Y.; Li, X. A Weakly Supervised Surface Defect Detection Based on Convolutional Neural Network. *IEEE Access* **2020**, *8*, 42285–42296. [CrossRef]
154. Huang, Y.; Qiu, C.; Wang, X.; Wang, S.; Yuan, K. A Compact Convolutional Neural Network for Surface Defect Inspection. *Sensors* **2020**, *20*, 1974. [CrossRef]
155. Scime, L.; Beuth, J. A multi-scale convolutional neural network for autonomous anomaly detection and classification in a laser powder bed fusion additive manufacturing process. *Addit. Manuf.* **2018**, *24*, 273–286. [CrossRef]
156. Chen, Y.; Wang, H.; Wu, Y.; Wang, H. Predicting the Printability in Selective Laser Melting with a Supervised Machine Learning Method. *Materials* **2020**, *13*, 5063. [CrossRef]
157. Huang, D.J.; Li, H. A machine learning guided investigation of quality repeatability in metal laser powder bed fusion additive manufacturing. *Mater. Des.* **2021**, *203*, 109606. [CrossRef]
158. Nguyen, N.V.; Hum, A.J.W.; Tran, T. A semi-supervised machine learning approach for in-process monitoring of laser powder bed fusion. In Proceedings of the The International Conference on Additive Manufacturing for a Better World, Changi, Singapore, 23–25 August 2022.
159. Nguyen, N.V.; Hum, A.J.W.; Do, T.; Tran, T. Semi-supervised machine learning of optical in-situ monitoring data for anomaly detection in laser powder bed fusion. *Virtual Phys. Prototyp.* **2023**, *18*, e2129396. [CrossRef]
160. Okaro, I.A.; Jayasinghe, S.; Sutcliffe, C.; Black, K.; Paoletti, P.; Green, P.L. Automatic fault detection for laser powder-bed fusion using semi-supervised machine learning. *Addit. Manuf.* **2019**, *27*, 42–53. [CrossRef]
161. Mitchell, J.A.; Ivanoff, T.A.; Dagel, D.; Madison, J.D.; Jared, B. Linking pyrometry to porosity in additively manufactured metals. *Addit. Manuf.* **2020**, *31*, 100946. [CrossRef]
162. Scime, L.; Beuth, J. Using machine learning to identify in-situ melt pool signatures indicative of flaw formation in a laser powder bed fusion additive manufacturing process. *Addit. Manuf.* **2019**, *25*, 151–165. [CrossRef]
163. Yuan, B.; Giera, B.; Guss, G.; Matthews, I.; Mcmains, S. Semi-Supervised Convolutional Neural Networks for In-Situ Video Monitoring of Selective Laser Melting. In Proceedings of the IEEE Winter Conference on Applications of Computer Vision (WACV), Waikoloa Village, HI, USA, 7–11 January 2019.
164. Larsen, S.; Hooper, P.A. Deep semi-supervised learning of dynamics for anomaly detection in laser powder bed fusion. *J. Intell. Manuf.* **2022**, *33*, 457–471. [CrossRef]
165. Pandiyan, V.; Drissi-Daoudi, R.; Shevchik, S.; Masinelli, G.; Le-Quang, T.; Loge, R.; Wasmer, K. Semi-supervised Monitoring of Laser powder bed fusion process based on acoustic emissions. *Virtual Phys. Prototyp.* **2021**, *16*, 481–497. [CrossRef]
166. Gondara, L. Medical Image Denoising Using Convolutional Denoising Autoencoders. In Proceedings of the IEEE 16th International Conference on Data Mining Workshops (ICDMW), Barcelona, Spain, 12–15 December 2016.
167. Mahmud, M.S.; Huang, J.Z.; Fu, X. Variational Autoencoder-Based Dimensionality Reduction for High-Dimensional Small-Sample Data Classification. *Int. J. Comput. Intell. Appl.* **2020**, *19*, 2050002. [CrossRef]
168. Hahn, T.V.; Mechefske, C.K. Self-supervised learning for tool wear monitoring with a disentangled-variational-autoencoder. *Int. J. Hydromechatron.* **2021**, *4*, 69–98. [CrossRef]
169. Schlegl, T.; Seeböck, P.; Waldstein, S.M.; Langs, G.; Schmidt-Erfurth, U. f-AnoGAN: Fast unsupervised anomaly detection with generative adversarial networks. *Med. Image Anal.* **2019**, *54*, 30–44. [CrossRef] [PubMed]
170. Mattera, G.; Polden, J.; Caggiano, A.; Nele, L.; Pan, Z.; Norrish, J. Semi-supervised learning for real-time anomaly detection in pulsed transfer wire arc additive manufacturing. *J. Manuf. Process.* **2024**, *128*, 84–97. [CrossRef]
171. Lui, C.F.; Maged, A.; Xie, M. A novel image feature based self-supervised learning model for effective quality inspection in additive manufacturing. *J. Intell. Manuf.* **2024**, *35*, 3542–3558. [CrossRef]
172. Wang, R.; Standfield, B.; Dou, C.; Law, A.C.; Kong, Z.J. Real-time process monitoring and closed-loop control on laser power via a customized laser powder bed fusion platform. *Addit. Manuf.* **2023**, *66*, 103449. [CrossRef]
173. Dharmawan, A.G.; Xiong, Y.; Foong, S.; Soh, G.S. A Model-Based Reinforcement Learning and Correction Framework for Process Control of Robotic Wire Arc Additive Manufacturing. In Proceedings of the IEEE International Conference on Robotics and Automation (ICRA), Virtual, 31 May–31 August 2020.
174. Knaak, C.; Masseling, L.; Duong, E.; Abels, P.; Gillner, A. Improving Build Quality in Laser Powder Bed Fusion Using High Dynamic Range Imaging and Model-Based Reinforcement Learning. *IEEE Access* **2021**, *9*, 55214–55231. [CrossRef]
175. Ogoke, F.; Farimani, A.B. Thermal control of laser powder bed fusion using deep reinforcement learning. *Addit. Manuf.* **2021**, *46*, 102033. [CrossRef]
176. Yeung, H.; Lane, B.M.; Donmez, M.A.; Fox, J.C.; Neira, J. Implementation of Advanced Laser Control Strategies for Powder Bed Fusion Systems. In Proceedings of the 46th SME North American Manufacturing Research Conference, College Station, TX, USA, 18–22 June 2018.

177. Shi, S.; Liu, X.; Wang, Z.; Chang, H.; Wu, Y.; Yang, R.; Zhai, Z. An intelligent process parameters optimization approach for directed energy deposition of nickel-based alloys using deep reinforcement learning. *J. Manuf. Process.* **2024**, *120*, 1130–1140. [CrossRef]
178. Rosenthal, D. Mathematical Theory of Heat Distribution during Welding and Cutting. *Weld. J.* **1941**, *20*, 220–234.
179. Dharmadhikari, S.; Menon, N.; Basak, A. A reinforcement learning approach for process parameter optimization in additive manufacturing. *Addit. Manuf.* **2023**, *71*, 103556. [CrossRef]
180. Eagar, T.W.; Tsai, N.S. Temperature Fields Produced by Travelling Distributed Heat Sources. *Weld. J.* **1983**, *62*, 346–355. [CrossRef]
181. Chung, J.; Shen, B.; Law, A.C.C.; Kong, Z. Reinforcement learning-based defect mitigation for quality assurance of additive manufacturing. *J. Manuf. Syst.* **2022**, *65*, 822–835. [CrossRef]
182. Mohamed, A.F.; Careri, F.; Khan, R.; Attallah, M.; Stella, L. A novel porosity prediction framework based on reinforcement learning for process parameter optimization in additive manufacturing. *Scr. Mater.* **2024**, *255*, 116377. [CrossRef]
183. Mattera, G.; Caggiano, A.; Nele, L. Optimal data-driven control of manufacturing processes using reinforcement learning: An application to wire arc additive manufacturing. *J. Intell. Manuf.* **2024**, 1–20. [CrossRef]
184. Wang, L.; Pan, Z.; Wang, J. A review of reinforcement learning based intelligent optimization for manufacturing scheduling. *Complex Syst. Model. Simul.* **2021**, *1*, 257–270. [CrossRef]
185. Alicastro, M.; Ferone, D.; Festa, P.; Fugaro, S.; Pastore, T. A reinforcement learning iterated local search for makespan minimization in additive manufacturing machine scheduling problems. *Comput. Oper. Res.* **2021**, *131*, 105272. [CrossRef]
186. Ying, K.C.; Lin, S.W. Minimizing makespan in two-stage assembly additive manufacturing: A reinforcement learning iterated greedy algorithm. *Appl. Soft Comput.* **2023**, *138*, 110190. [CrossRef]
187. Kucukkoc, I. MILP models to minimize makespan in additive manufacturing machine scheduling problems. *Comput. Oper. Res.* **2019**, *105*, 58–67. [CrossRef]
188. Li, Q.; Kucukkoc, I.; Zhang, D.Z. Production planning in additive manufacturing and 3D printing. *Comput. Oper. Res.* **2017**, *83*, 157–172. [CrossRef]
189. Sun, M.; Ding, J.; Zhao, Z.; Chen, J.; Huang, G.; Wang, L. Out-of-order execution enabled deep reinforcement learning for dynamic additive manufacturing scheduling. *Robot. Comput. Integr. Manuf.* **2024**, *91*, 102841. [CrossRef]
190. Yang, Y.; Yang, L.; Farrag, A.; Ning, F.; Jin, Y. Multi-laser scan assignment and scheduling optimization for large-scale metal additive manufacturing. *IISE Trans.* **2024**, 1–16. [CrossRef]